NORTHWEST FISHERIES CENTER
PROCESSED REPORT
JULY 1976

TIDAL CURRENTS AND POLLUTANT DISPERSAL IN THE WESTERN GULF OF ALASKA AS DERIVED FROM A HYDRODYNAMICAL-NUMERICAL MODEL

by

John M. Harding

Prepared by:
Northwest Fisheries Center
National Marine Fisheries Service
2725 Montlake Boulevard E.
Seattle, Washington 98112

NOTICE

TIDAL CURRENTS AND POLLUTANT DISPERSAL IN THE WESTERN GULF OF ALASKA AS DERIVED FROM A HYDRODYNAMICAL-NUMERICAL MODEL

by

John M. Harding

Northwest Fisheries Center
National Marine Fisheries Service
National Oceanic and Atmospheric Administration
2725 Montlake Boulevard East
Seattle, Washington 98112

July 1976

CONTENTS

LIST OF FIGURES

1. INTRODUCTION

The computation of tides and currents using hydrodynamical-numerical (HN) models was originally proposed in 1938 by Professor Walter Hansen of the University of Hamburg. However, it was not until the advent of the electronic computer that this approach became feasible. These models, based on the equations of motion modified to operate on vertically integrated mass transport, have been well tested over the past 20 years for single-layer cases. Since 1967, in collaboration with Professor Hansen, Dr. Taivo Laevastu of the Oceanography Department, Naval Environmental Prediction Research Facility, has extended these models to allow multiple open boundaries, multiple layers, and various auxiliary computations [1-5]. The analysis and prediction of advection and diffusion of pollutants is easily incorporated into the HN formulation since current components are computed in short time intervals.

An optimized multilayer HN model [6], in two-layer mode, was applied to three overlapping areas in the Gulf of Alaska. The results described here concern the westernmost grid which extends along the Alaskan Peninsula from eastern Kodiak Island, southwestward to Unimak Pass and offshore to an approximate distance of 300 km (Figure 1).

The project was funded by the Outer Continental Shelf Energy Project of NOAA. The Project Officer was Dr. Mauri Pelto, OCSEP office of NOAA. Appreciation is expressed to the following members of the NEPRF staff for the technical support services noted: Mrs. P. Mousseau and Mrs. W. Carlisle, manuscript typing; Mr. R. Clark, graphics; Mr. S. Myrick, photography; and Mr. S. Bishop, editing.

2. THE EQUATION SET

The basic set of equations includes: (a) vertically integrated equations of motion for each layer; (b) two interdependent continuity equations, one for each layer; and (c) the equations setting the boundary conditions.

(a) Equations of Motion:

$$\dot{U}1 + \frac{r\sqrt{U1^2 + V1^2}}{H_u} U1 - fV1 + g\zeta_{1x} = K^{(x)}$$

$$\dot{V}1 + \frac{r\sqrt{U1^2 + V1^2}}{H_{v1}} V1 + fU1 + g\zeta_{1y} = K^{(y)} \qquad \text{(Layer 1)}$$

$$\dot{U}2 + \frac{r\sqrt{U2^2 + V2^2}}{H_{u2}} U2 - fV2 + g\frac{\rho_1}{\rho_2}\zeta_{1x} +$$

$$g\left(1 - \frac{\rho_1}{\rho_2}\right)\zeta_{2x} = 0$$

$$\dot{V}2 + \frac{r\sqrt{U2^2 + V2^2}}{H_{v2}} V2 + fU2 + g\frac{\rho_1}{\rho_2}\zeta_{1y} + \qquad \text{(Layer 2)}$$

$$g\left(1 - \frac{\rho_1}{\rho_2}\right)\zeta_{2y} = 0$$

(b) Continuity Equations:

$$\dot{\zeta}_1 - \dot{\zeta}_2 + (H_1\ U1)_x + (H_1\ V1)_y = 0 \qquad \text{(Layer 1)}$$

$$\dot{\zeta}_2 + (H_2\ U2)_x + (H_2\ V2)_y = 0 \qquad \text{(Layer 2)}$$

where:

ζ_1 = surface elevation

ζ_2 = deviation of MLD (mixed layer depth) from its mean (initially prescribed) depth

U1, V1 = u,v components in first layer

U2, V2 = u,v components in second layer

r = friction coefficient (internal friction)

f = Coriolis parameter

r_b = bottom friction coefficient

g = acceleration of gravity

H = layer thickness

ρ_1, ρ_2 = densities of the respective layers

$K^{(x)}$, $K^{(y)}$ = external forces

$(\ )_x$ = partial with respect to x = $\frac{\partial(\ )}{\partial x}$

Detailed descriptions of these equations as well as their finite difference formulations are available in [1].

(c) Boundary Conditions

For the two-layer mode of the optimized HN model used in the Gulf of Alaska region, the boundary conditions were: (1) No normal flow at land-sea boundaries; and (2) flow through open boundaries, as computed internally one grid distance from the boundary.

Wind stress on the surface layer was parameterized using

$$\tau(x) = \lambda \frac{\omega_x \sqrt{\omega_x^2 + \omega_y^2}}{H}$$

$$\tau(y) = \lambda \frac{\omega_y \sqrt{\omega_x^2 + \omega_y^2}}{H}$$

where:

λ = the drag coefficient

ω = the wind speed

ω_x, ω_y = components of wind vector

$\tau(x), \tau(y)$ = components of the stress vector

Water surface elevations of several grid boundary locations were specified as the driving force for tidal currents within the area. Because of a lack of actual tidal data along the boundaries, values from Kodiak Island and Sanak Island were utilized as described below and depicted in Figure 4.

Kodiak tides were used along the Shelikof Straits boundary and Sanak tides were used through the Unimak Pass. For the offshore oceanic grid boundary parallel to the Alaska Peninsula, a linearly interpolated tide from southwest to northeast was specified using Sanak tides at the westernmost corner and Kodiak tides at the easternmost corner. The amplitude, phase speed and phase angle of each component of the Sanak and Kodiak tides are given in Table 1. The eastern grid boundary south of Kodiak and the western grid boundary are not externally forced. Due to the extreme thickness of the second layer (relative to the first) over the Aleutian

Table 1. Values of tidal components.

Location	Component	Amplitude (cm)	Phase Angle (deg)	Phase Speed (deg/hr)
Kodiak Is. 57°47'N 152°24'W	M_2	98.4	8	28.984
	K_1	40.5	139	15.041
	O_1	27.3	122	13.943
	S_2	32.8	41	30.000
Sanak Is. 54°23'N 162°38'W	M_2	58.6	355	28.984
	K_1	41.6	124	15.041
	O_1	23.6	97	13.943
	S_2	22.1	18	30.000

Trench, water surface elevations specified at the forced boundaries were assumed to result solely from tidally induced variations in the thickness of the second layer. A general and more complete discussion of boundary conditions for HN models can be found in Kagan [7].

3. DIFFUSION AND ADVECTION [1]

Diffusion in water bodies has been presented in many formulas, a few of which are given here (neglecting vertical diffusion).

The general diffusion formula is

$$\frac{\partial^2 S}{\partial x^2} + \frac{\partial^2 S}{\partial y^2} - \frac{1}{A}\frac{\partial S}{\partial t} = 0 \ ;$$

the basic dispersion formula is

$$\frac{\partial S}{\partial t} = Y - \frac{S}{n} - \frac{\partial}{\partial x}(U_x + pS_x) - \frac{\partial}{\partial y}(U_y + pS_y) \ ;$$

and the Fickian equation is

$$\frac{\partial S}{\partial t} = Y - \frac{S}{n} + K\nabla^2 S - \frac{\partial}{\partial x}(S_u U) - \frac{\partial}{\partial y}(S_v V);$$

where:

Y = addition (release)
n = decay
S = concentration
$pS_{x,y}$ = concentration velocity component
t = time
K (coefficient) = $\beta a v_r$ (a = depth; $v_r = u^2 + v^2$; $\beta = 0.003$)
S_u, S_v = concentration gradients in u and v direction
A = diffusion coefficient (Austausch coefficient)

The Lagrangian approach of diffusion in finite difference form was adopted by Wolff, Hansen and Joseph [8]:

$$S^{t+\tau}_{n,m} = S^t_{n,m}\left(1 - \frac{4\tau A}{\ell^2}\right) + \frac{A\tau}{\ell^2}\left(S^t_{n-1,m} + S^t_{n+1,m} + S^t_{n,m-1} + S^t_{n,m+1} - 4S^t_{n,m}\right)$$

where:

t = time
τ = time step
ℓ = grid size
S = concentration
A = diffusion coefficient
n,m = grid coordinates

The above finite equation deviates from the usual finite difference diffusion formula only in the addition of the last term (-4S), which makes the solution similar to the solution of the "Laplacian" ($K\nabla^2 S$). Also, the advection is computed linearly in finite difference form:

$$S^{t+\tau}_{n,m} = S^{t}_{n,m} - \tau \left| U^{t+\tau}_{n,m} \right| \frac{(S^{t}_{n,m} - S^{t}_{n,m\pm1})}{\ell} -$$

$$- \tau \left| V^{t+\tau}_{n,m} \right| \frac{(S^{t}_{n,m} - S^{t}_{n\pm1,m})}{\ell}$$

where Sn,m-1 or n,m+1 (respectively n-1, n+1) are used, depending on the direction (sign) of U and V.

The Lagrangian approach used by Wolff, Hansen and Joseph [8], though reproducing the diffusion process well, does not conserve absolutely the amount of the dispersing substance. The following modified formula, however, was found to be conservative, provided the proper A (Austausch coefficient) is chosen and corresponds to the chosen time step and grid size:

$$S^{t+\tau}_{n,m} = S^{t}_{n,m} - \frac{4\tau A}{\ell^2} S^{t}_{n,m} + \frac{\tau A}{\ell^2} (S^{t}_{n-1,m} + S^{t}_{n,m-1}$$

$$+ S^{t}_{n+1,m} + S^{t}_{n,m+1} - 4S^{t}_{n,m}) + \frac{\tau A}{\ell^2} (S^{t}_{n-1,m-1}$$

$$+ S^{t}_{n-1,m+1} + S^{t}_{(n+1,m-1)} + S^{t}_{(n+1,m+1)})$$

It should be mentioned that the transport equation used in NEPRF programs is very similar to the "upwind" difference scheme used in air pollution problems (Pandolfo et al. [9]). This scheme requires that $\frac{U\Delta t}{\Delta \ell} < 1$.

The Austausch coefficient (A) is a function of grid size and time step. In an experiment designed to investigate the conservation of diffusing substances, one of the main criteria was found to be a relationship between grid size and time step. This relation of A to grid size with a 1,000 sec time step is shown in Figure 2. The correct value of A is found from this graph and from the relation, $A = \frac{1,000}{\Delta t} A$ (graph). With a small time step, the value of A approaches that found empirically by Okubo and Ozmidov [10] and Kullenberg [11]. An idea of the proper A to be used in different grid sizes can be obtained also from the Joseph and Sendner [12] formulation. There is still some slight uncertainty about the dependence of the horizontal Austausch coefficient (K_h) on the length scale, $K_H = k_1 \times 10^{-3} \ell^{k2}$. Kullenberg [11] gives the values for the coefficients $k_1 = 1.3$ and $k_2 = 1.31$, whereas Okubo [13] gives the corresponding values as 1.03 and 1.15. Both lines are shown in Figure 2.

4. INPUTS AND RESULTS

Case 1 is a 48-hour, tides-only (no wind) run. Beginning at approximately high tide, hour 29 (104400 s), a continuous source of pollutants is input at row 12, column 47, approximately 56°50'N, 155°W (Figure 1). The amount of continuous source is 1000 units/day, input into the model as 0.463 units per 40-second time step. Case 1 is considered to be a summer case with the thickness of the first layer (mixed layer depth) as 20 m.

A time series of layer 1 surface currents (cm/s) and tidal heights (cm) at point 12,47 for Case 1 is given in Figure 6. The circled times on the x-axis are those at which layer 1 and 2 currents (cm/s) and height deviations (cm) are presented over the whole grid (Figures 7 through 15).

Case 2 is indentical to Case 1 except a constant wind of 10 m/s from 320° true is used to force the surface layer over the whole grid. The wind is started at hour 24 (86400 s) and is continued through the remainder of the run. Considering current flow during the no-winds condition, winds from 320° true were chosen as a worst case situation with respect to pollutant landfall originating from a source at point 12,47.

Figure 16 is a time series of layer 1 surface currents (cm/s) and tidal heights (cm) at point 12,47 for Case 2. Circled times on the x-axis are those for which layer 1 and 2 currents (cm/s) and height deviations (cm) are presented over the entire grid (Figures 17 through 25). Pollutant distribution at hours 42 and 48, after initializing the continuous source at hour 29, are shown in Figures 26 and 27 for Cases 1 and 2 respectively.

In Figures 7-15 and 17-27, contour intervals are as follows: layer 1 plots, 5 cm; layer 2 plots, 50 cm; and pollutant plots, 200 arbitrary units. Layer 1 and 2 currents are represented by current barbs at every-other grid point. Each flag on a current barb indicates 10 cm/s; thus a barb with two and one-half flags represents a current of 25 cm/s (approximately one-half knot).

Values of the various constants input into this particular Gulf of Alaska model are given in Table 2.

Table 2. Constant parameters for computations of flow in the western Gulf of Alaska.

Constants	Values
Number of Rows Number of Columns	21 60
Grid Step (cm) Rotation Angle* (deg)	1481600 39
Wind Drag Coefficient Mid-latitude of Grid (deg)	3.2×10^{-6} 55.5
Bottom Friction Coefficient Austausch Coefficient	0.003_5 5.25×10^5
Time Step (sec) Number of Layers	40 2
Layer 1 Smoothing Parameter Layer 2 Smoothing Parameter	0.99 0.98
Layer 1 Density (gr/cm^3) Layer 2 Density (gr/cm^3)	1.023 1.025

*Counterclockwise angle between north and positive Y axis of the computational grid

5. VERIFICATION AND DISCUSSION

The work of Favorite et al. [14] describes surface flow in the vicinity of Kodiak Island using dynamic methods to obtain geostrophic currents. These methods, however, do not intrinsically resolve the tidal currents and currents due to sea level fluctuations which dominate in coastal waters.

Until adequate current measurements are obtained so that proper tuning and verification of the western grid Gulf of Alaska model can be accomplished, previously used and less satisfactory verification methods must be employed [5].

A harmonic prediction of surface heights, based on tidal station data within the grid but not used to drive the model, is compared to computed model output (Case 1) for the given location. Figure 5 demonstrates the comparison of a harmonic prediction from King Cove (55°04'N, 162°19'W) and computed data from row 5, column 15; it indicates good agreement between the harmonic prediction and computed data.

Three features should be noted in the current and height fields of Figures 7-15 and 17-25: (1) the extremes in surface height deviation (layer 1) off the southwest edge (row 9, column 9) of Sanak Island; (2) the apparent convergence zone (except in Case 2, layer 1) in the Shelikof Strait off the western tip of Kodiak Island; and (3) the apparent incoherence of the second layer height deviations.

The first feature off Sanak Island is probably caused by the juxtaposition of steep bottom topography arising out of the Aleutian Trench (Figure 3) and the relatively shallow bank to the southwest of Sanak.

The second feature, which appears in all but the winds case layer 1, is probably also due to bottom topography. Off the western corner of Kodiak Island, the 200 m contour (Figure 3) indicates a narrow channel which originates from the Aleutian Trench to the south and into but not completely through the Shelikof Straits. Further support of this feature off Kodiak is found in drift bottle studies [15] which indicate this area as a convergence zone. Persistence of these features off Sanak and Kodiak Islands, using various boundary prescriptions of the tidal inputs, also indicates that these features are of topographic origin rather than simply interactive effects caused by the given boundary prescriptions.

The third feature, the irregularities of the second layer height deviations, are possibly caused by topographic effects, but they may just as likely be caused by insufficient tuning of the model by means of the second layer smoothing parameters.

It would be of interest to attempt verification of the three features noted above to evaluate the extent of further tuning required.

Study of the actual numerical output of pollutant distributions is necessary for the best understanding of the dispersion of a continuous pollutant source in Cases 1 and 2 described previously. An indication of the numerical outputs is given in the pollutant contour plots for hours 42 and 48 for Case 1 (Figure 26) and Case 2 (Figure 27).

A southwestward trend of pollutant movement is observed in both Cases 1 and 2 with this tendency accentuated as expected in the case that includes winds from the northwest. Pollutant landfall in Cases 1 and 2 from a release at point 12,47 apparently occurs in the Trinity Islands to the southwest of Kodiak at least 22 hours after the start of continuous pollutant release.

The cause of the apparent slow dispersal from this particular release point is reasonable when the current velocities and grid step are compared. If one assumes the maximum current speed of 30 cm/s at point 12,47 is constant in the area, the grid step of 1481600 cm yields a simple advection speed of 13.7 hours per grid step. Diffusion hastens the spreading somewhat, but the speed is not a sustained 30 cm/s and the direction is also variable. The combination of these factors yields the apparent slow pollutant dispersal.

REFERENCES

1. Laevastu, T., 1974: A vertically integrated hydrodynamical-numerical model (W. Hansen type), model description and operating/running instructions. Part 1 of a series of four reports. ENVPREDRSCHFAC Tech. Note No. 1-74.

2. Laevastu, T., 1974: A multilayer hydrodynamical-numerical model (W. Hansen type), model description and operating/running instructions. Part 2 of a series of four reports. ENVPREDRSCHFAC Tech. Note No. 2-74.

3. Laevastu, T. with M. Clancy and A. Stroud, 1974: Computation of tides, currents and dispersal of pollutants in lower bay and approaches to New York with fine and medium grid size hydrodynamical-numerical models. Part 3 of a series of four reports. ENVPREDRSCHFAC Tech. Note No. 3-74.

4. Laevastu, T. and R. Callaway with A. Stroud and M. Clancy, 1974: Computation of tides, currents, and dispersal of pollutants in New York Bight from Block Island to Atlantic City with large grid size, single and two-layer hydrodynamical-numerical models. Part 4 in a series of four reports. ENVPREDRSCHFAC Tech. Note No. 4-74.

5. Laevastu, T. and G. D. Hamilton, 1974: Computations of of real-time currents off Southern California with multilayer hydrodynamical-numerical models with several open boundaries. ENVPREDRSCHFAC Tech. Paper No. 15-74.

6. Bauer, R. A., 1974: Description of the optimized EPRF multilayer hydrodynamical-numerical model. ENVPREDRSCHFAC Tech. Paper No. 15-74.

7. Kagan, B. A., 1970: Properties of certain difference schemes used in the numerical solution of the equations for tidal motion. Izv. Atmos. and Ocean Phys., 6, 7, 704-717.

8. Wolff, P. M., W. Hansen and J. Joseph, 1970: Investigation and prediction of dispersion of pollutants in the sea with hydrodynamical-numerical (HN) models. Marine and Sealife (Fishing News, Ltd., London), 146-150.

9. Pandolfo, T. P., M. A. Atwater and G. E. Anderson, 1971: Prediction by numerical models of transport and diffusion in an urban boundary layer. Cent. Env. and Man, Inc., Hartford, CO, Rept. No. 4082, 139 pp.

10. Okubo, A., and R. V. Ozmidov, 1970: Empirical dependence of the coefficient of horizontal turbulent diffusion in the ocean on the scale of the phenomenon in question. Izv. Atmos. and Ocean Phys. 6, 5, 534-536.

11. Kullenberg, G., 1972: Apparent horizontal diffusion in stratified vertical shear flow. Tellus, 24, 17-28.

12. Joseph, J., and H. Sendner, 1958: Uber die horizontale diffusion im meere, Dtsch. Hydrogr, Zeitschr., 11, 2, 49-77.

13. Okubo, A., 1971: Oceanic diffusion diagrams. Deep Sea Res., 18, 8, 789-802.

14. Favorite, F., W. J. Ingraham, and D. M. Fisk, 1975: Environmental conditions near Portlock and Albatross Banks (Gulf of Alaska), May 1972. Northwest Fisheries Center Processed Dept., May.

15. Ingraham, W. J., A. Bakun, and F. Favorite, 1976: Physical oceanography of the Gulf of Alaska. Northwest Fisheries Center Processed Dept., March.

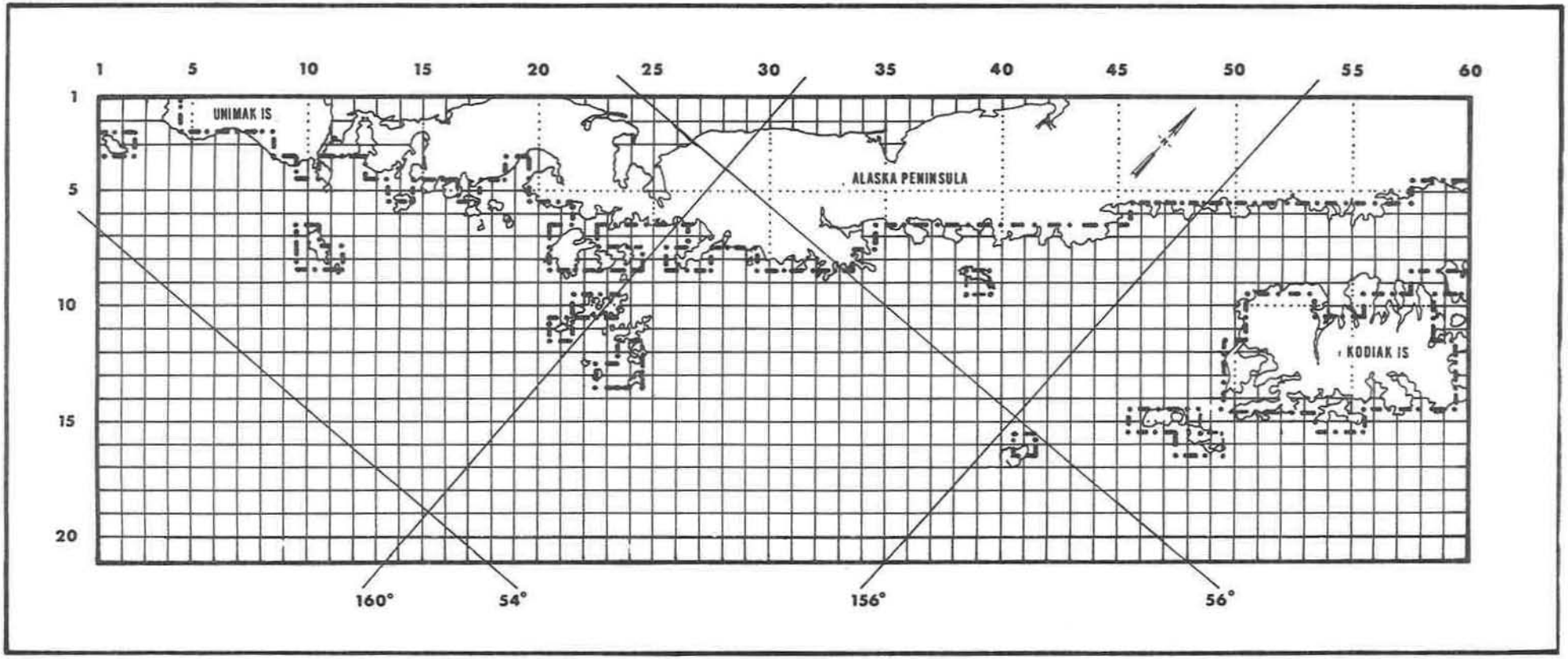

1. Gulf of Alaska, western grid.

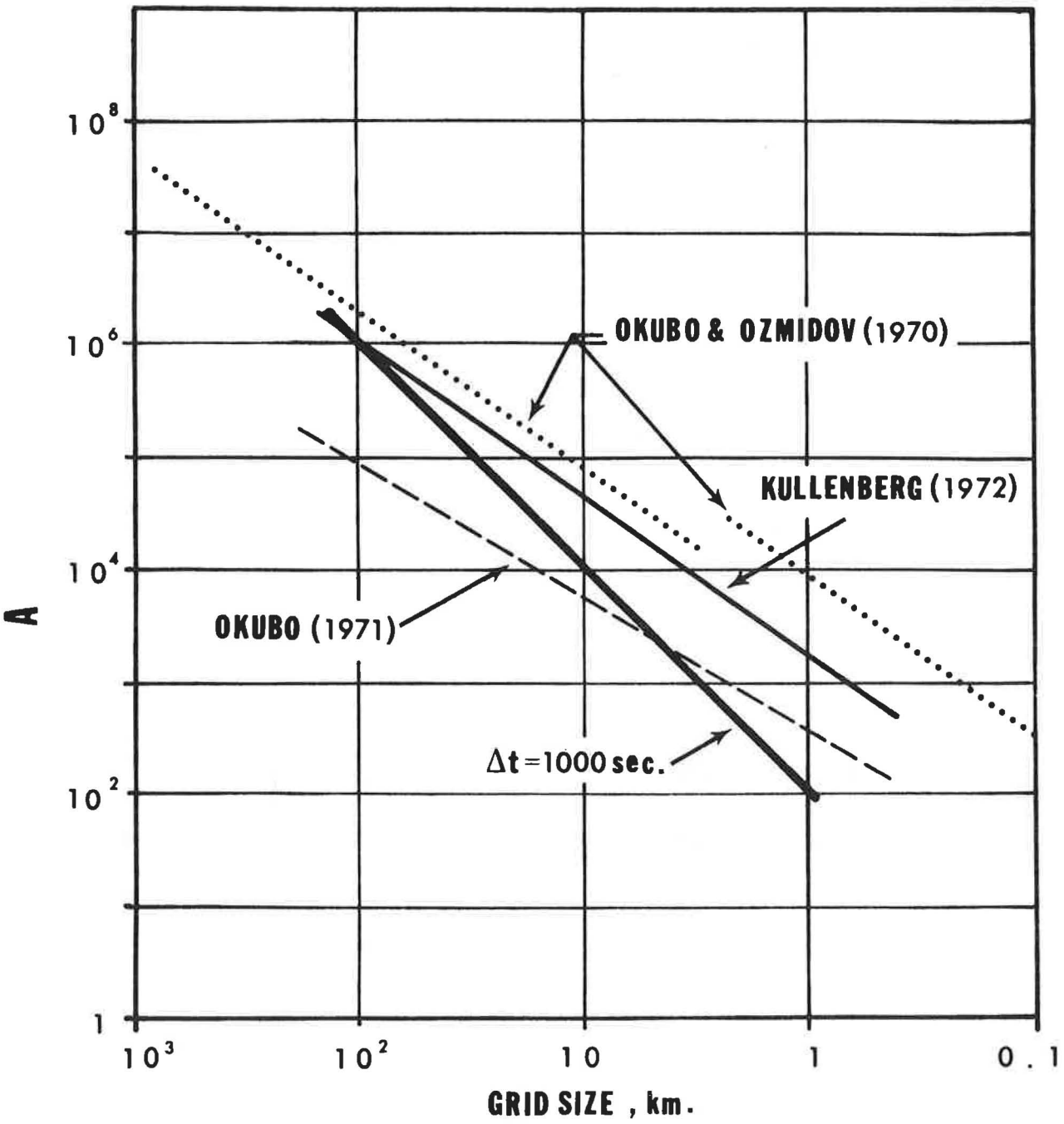

2. Austausch coefficient (A) vs. grid size (km) for t = 1000 s.

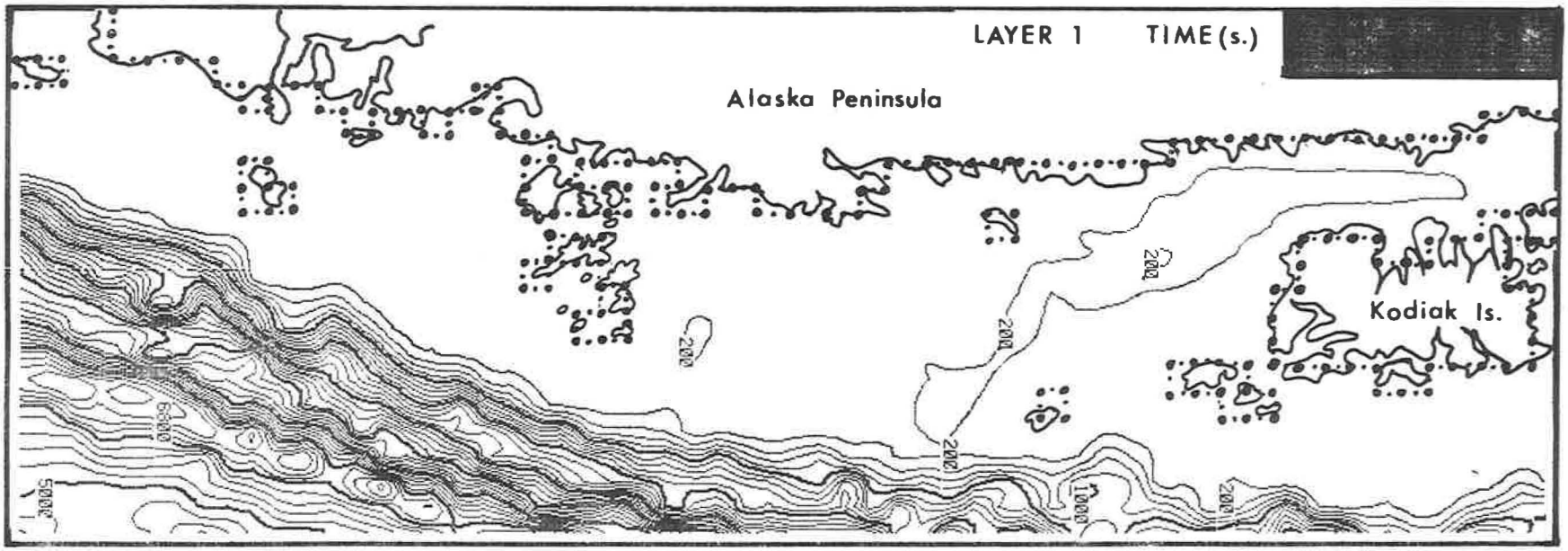

3. Bottom topography (m), Gulf of Alaska, western grid.

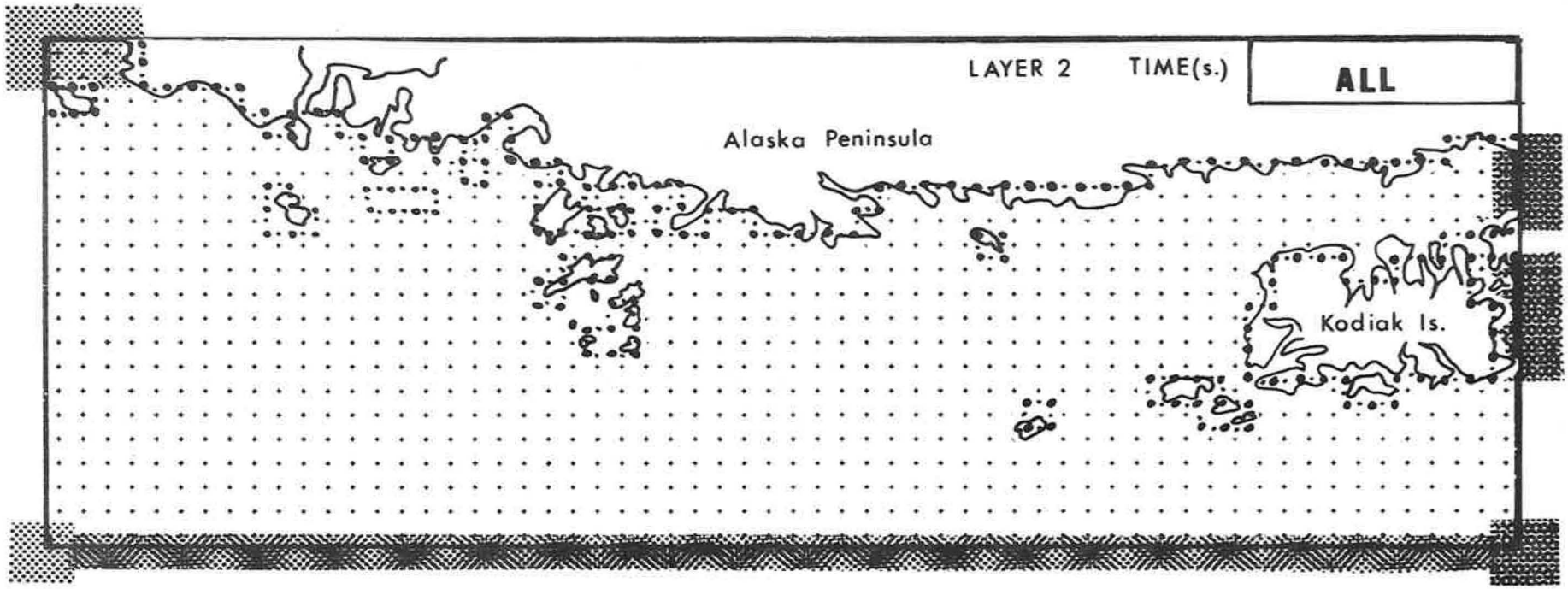

TIDAL INPUTS

SANAK ISLAND TIDES

SANAK / KODIAK INTERPOLATED TIDES

KODIAK TIDES

4. Tidal specifications at grid boundaries.

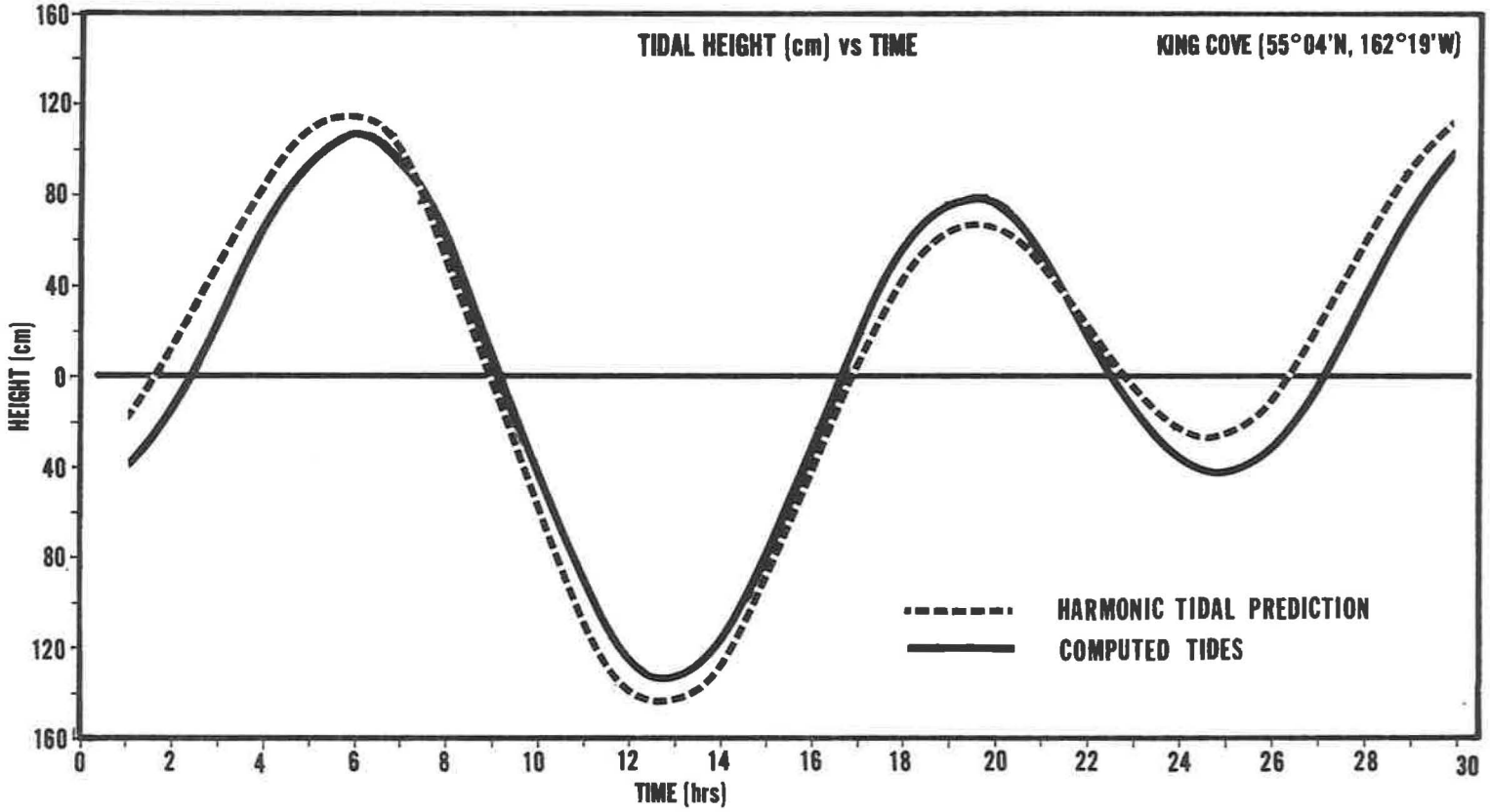

5. Harmonically predicted vs. computed tidal heights (cm) at King Cove (55°04'N, 162°19'N).

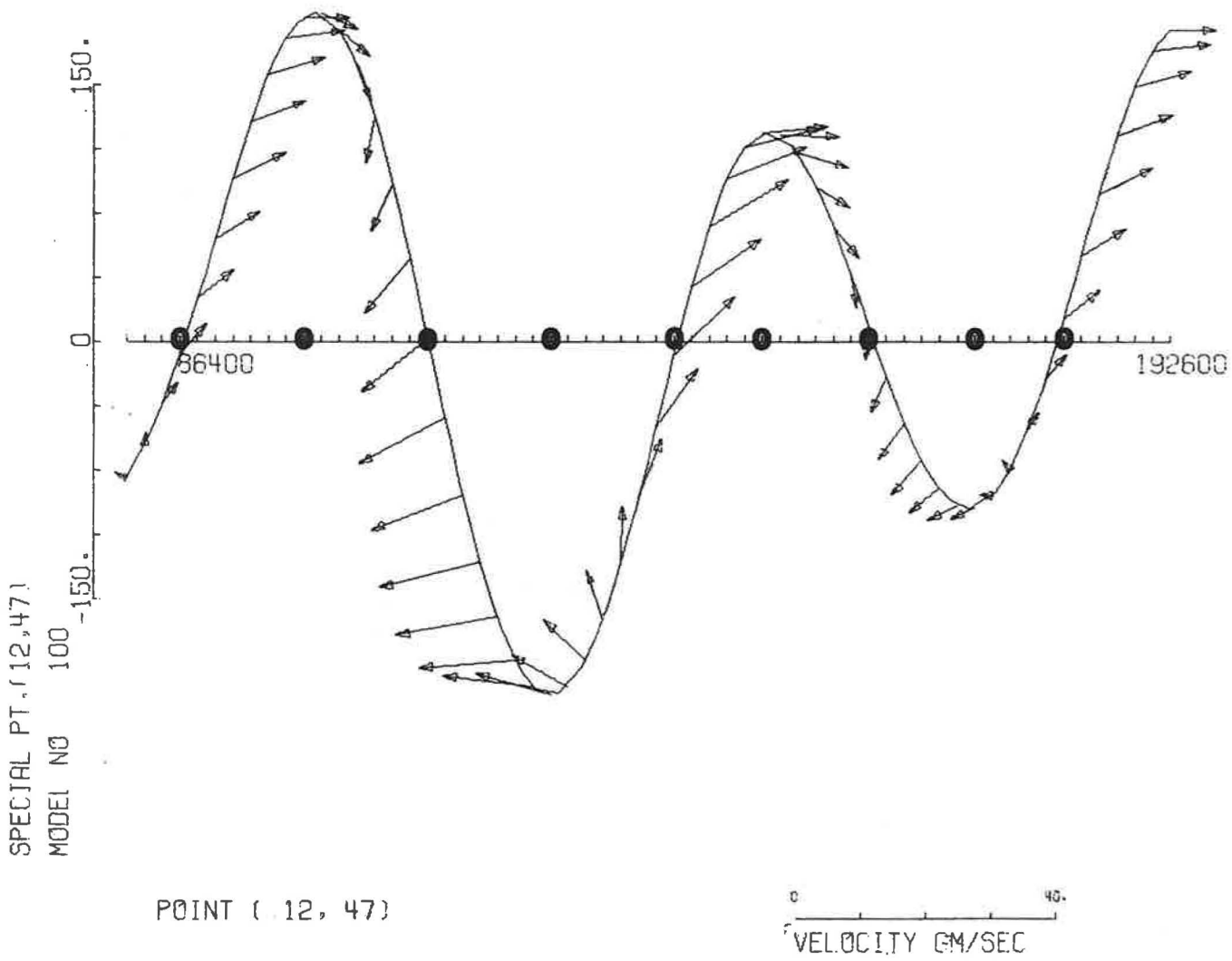

6. TIDAL HEIGHTS AND CURRENTS WITHOUT WINDS
LAYER3, OPTIMIZED H-N MODEL FOR B.L.M. GULF OF ALASKA, WESTERN GRID.

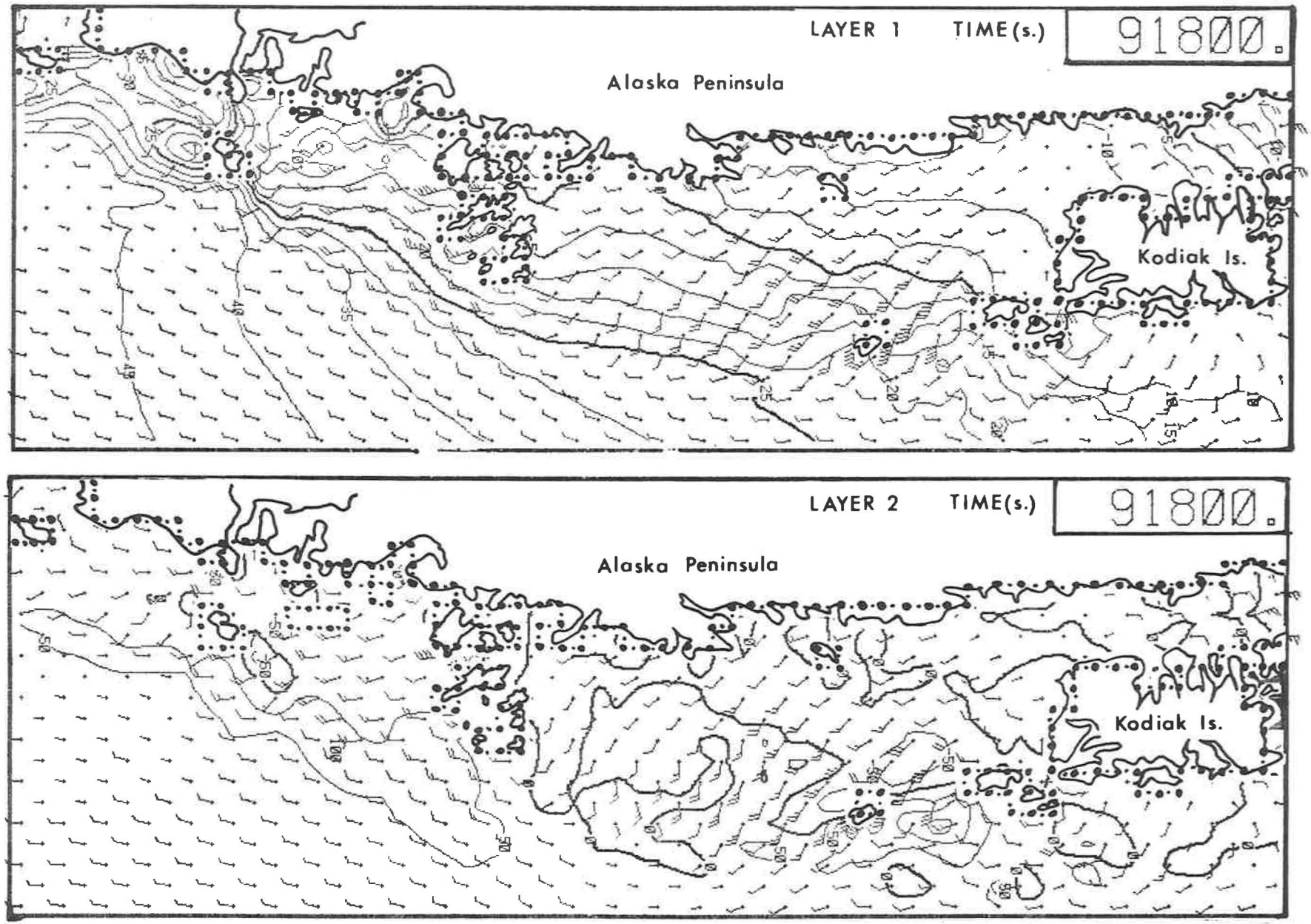

7. Case 1, currents (cm/s) and tidal heights (cm) for layers 1 and 2 at 25 1/2 hours (91800 s).

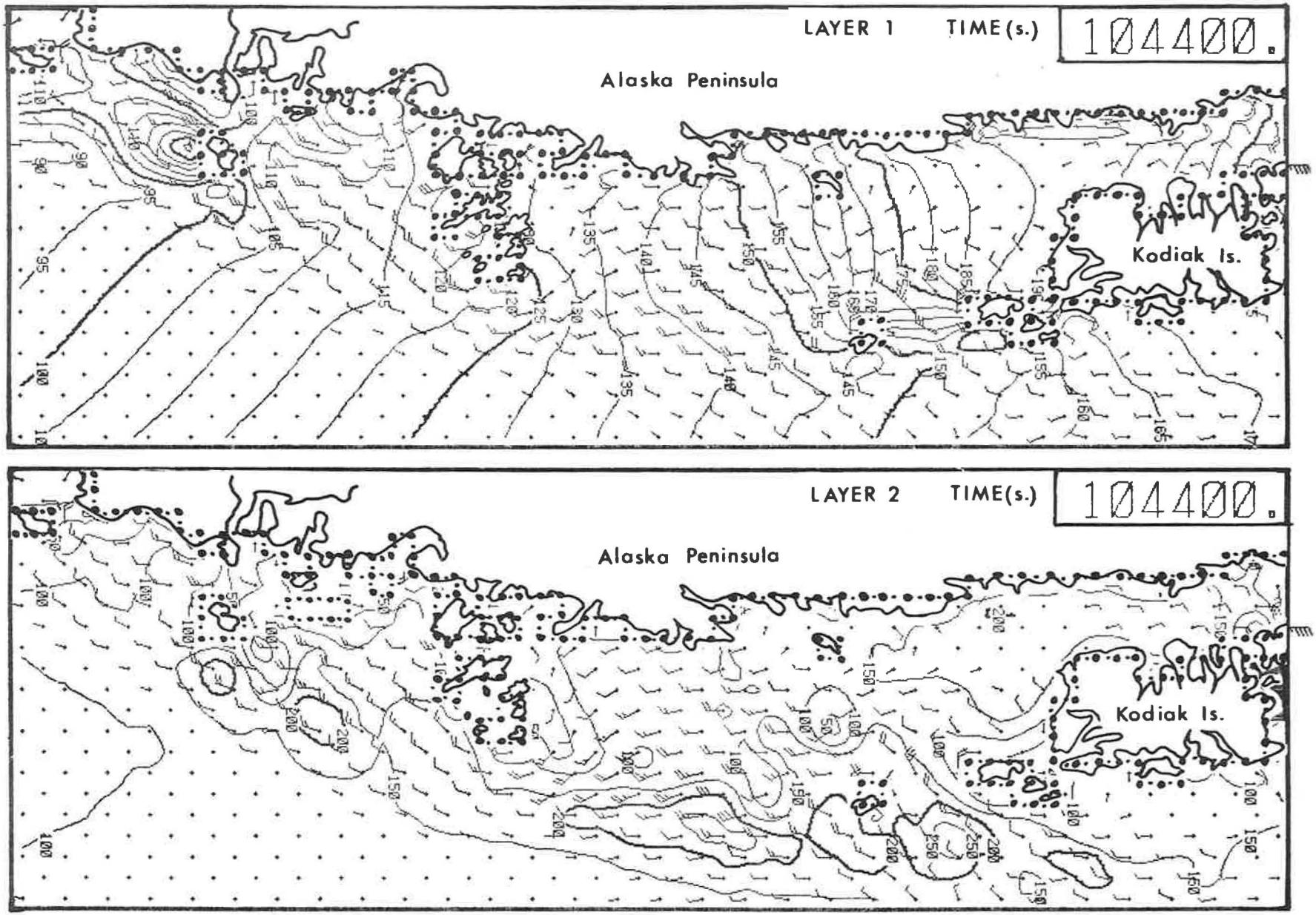

8. Case 1, currents (cm/s) and tidal heights (cm) for layers 1 and 2 at 29 hours (104400 s).

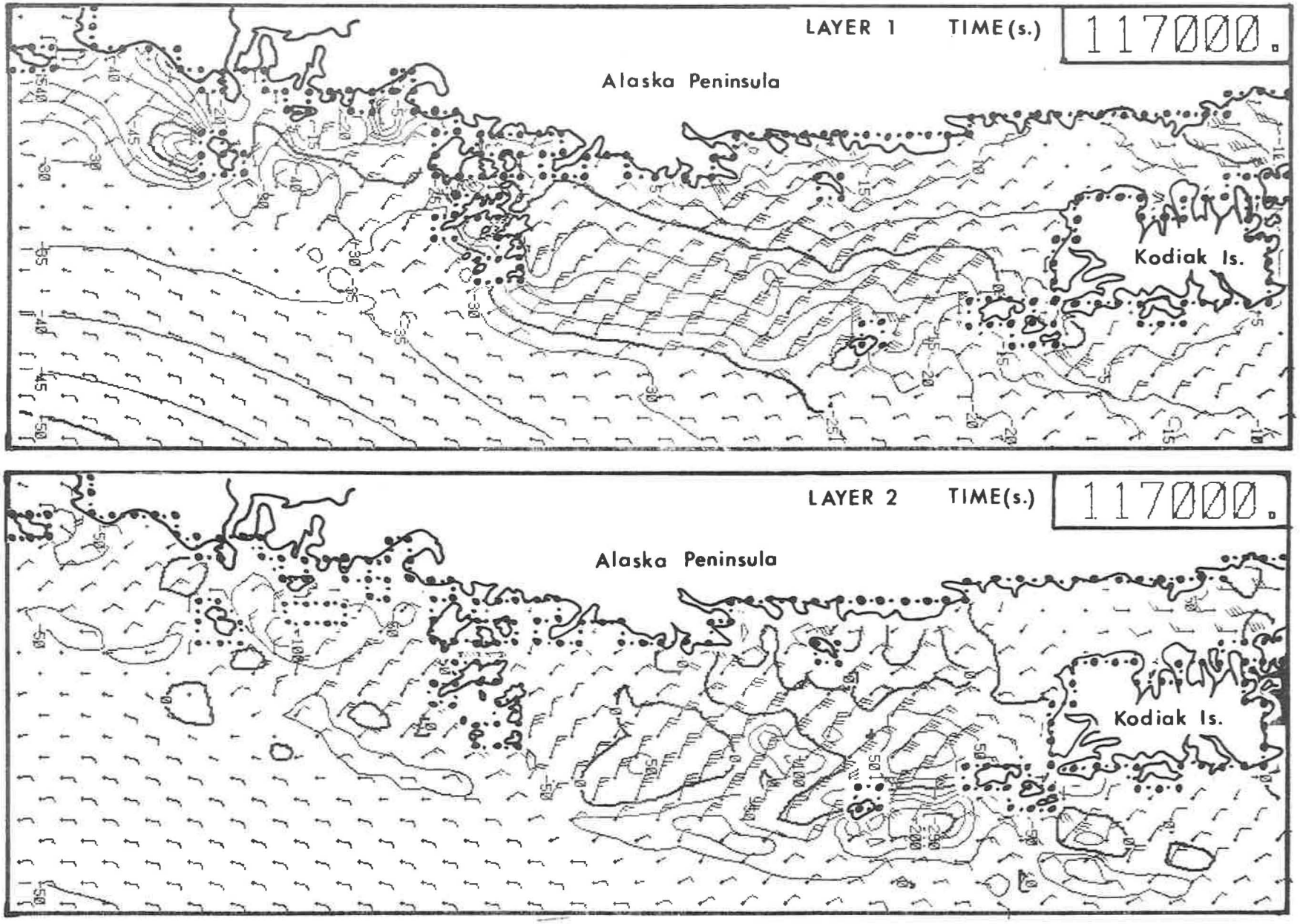

9. Case 1, currents (cm/s) and tidal heights (cm) for layers 1 and 2 at 32 1/2 hours (11700 s).

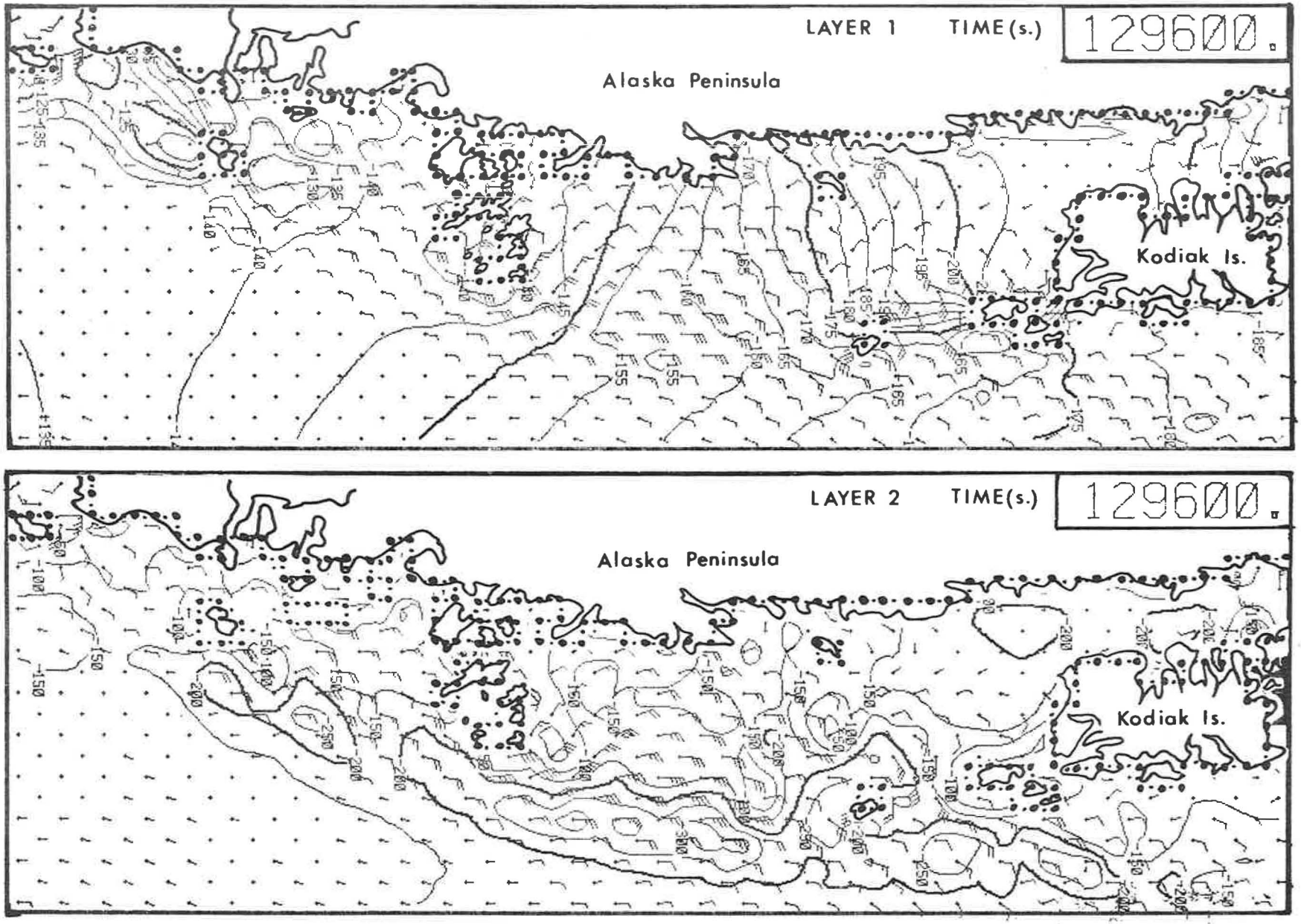

10. Case 1, currents (cm/s) and tidal heights (cm) for layers 1 and 2 at 36 hours (129600 s).

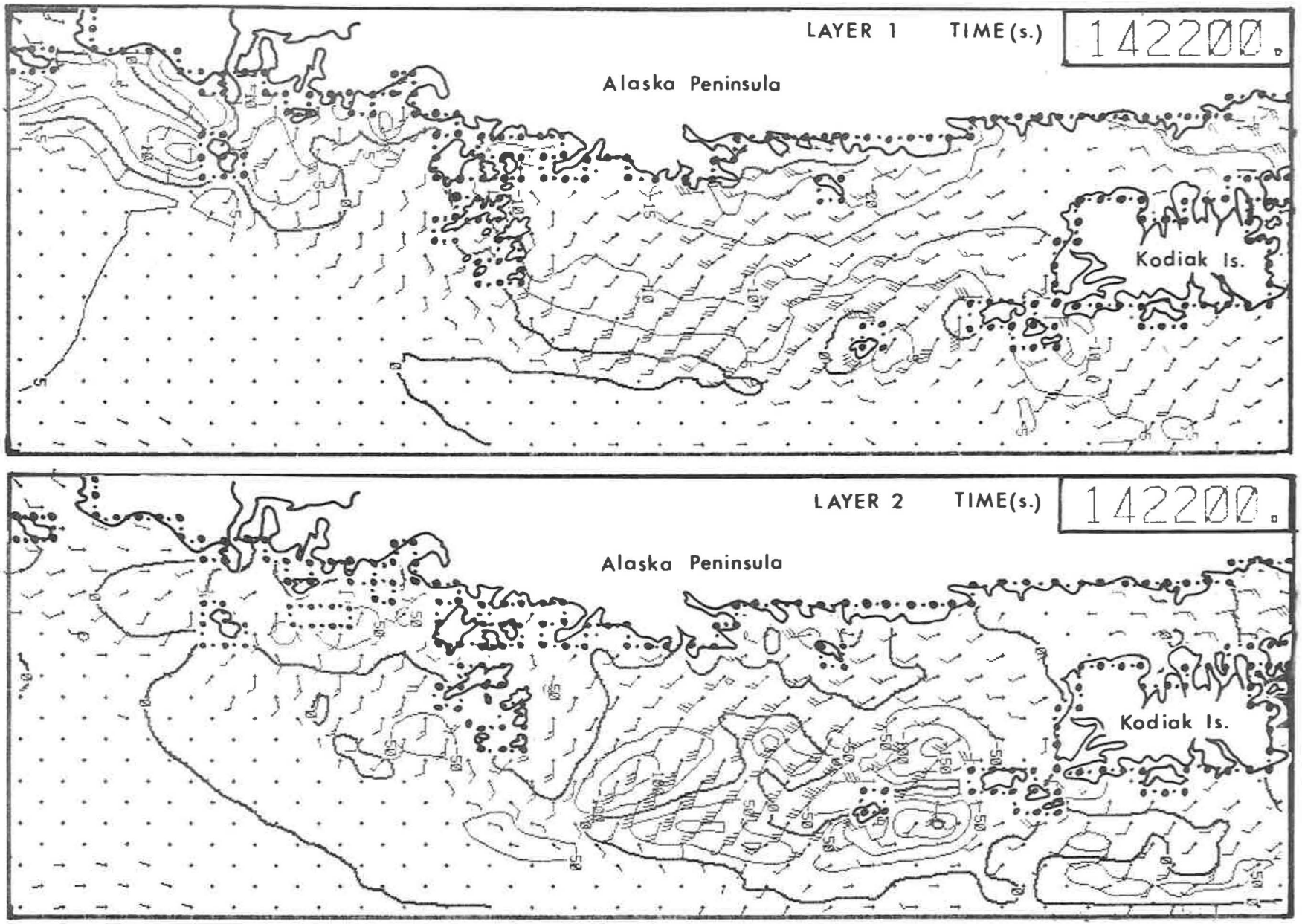

11. Case 1, currents (cm/s) and tidal heights (cm) for layers 1 and 2 at 39 1/2 hours (142200 s).

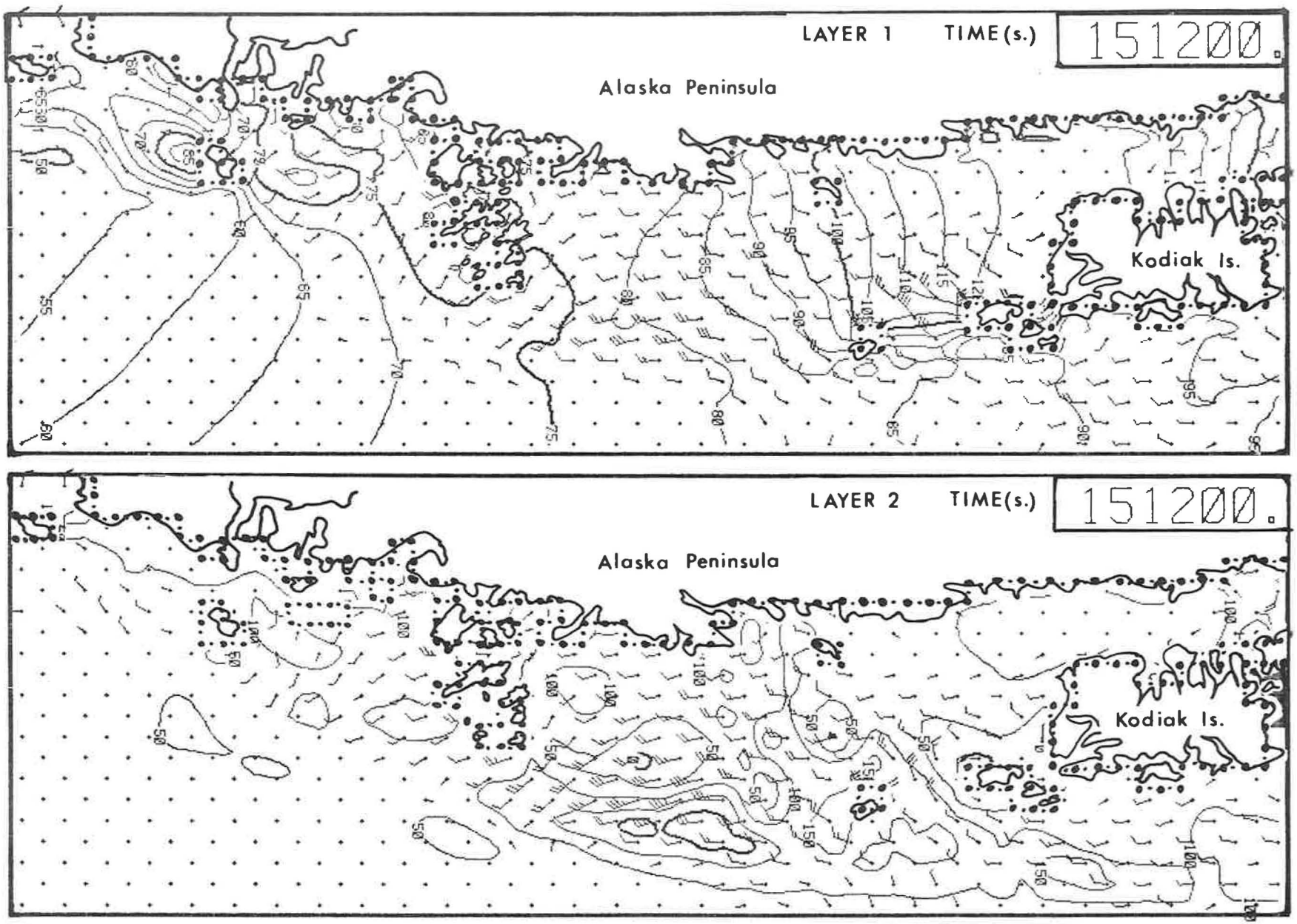

12. Case 1, currents (cm/s) and tidal heights (cm) for layers 1 and 2 at 42 hours (151200 s).

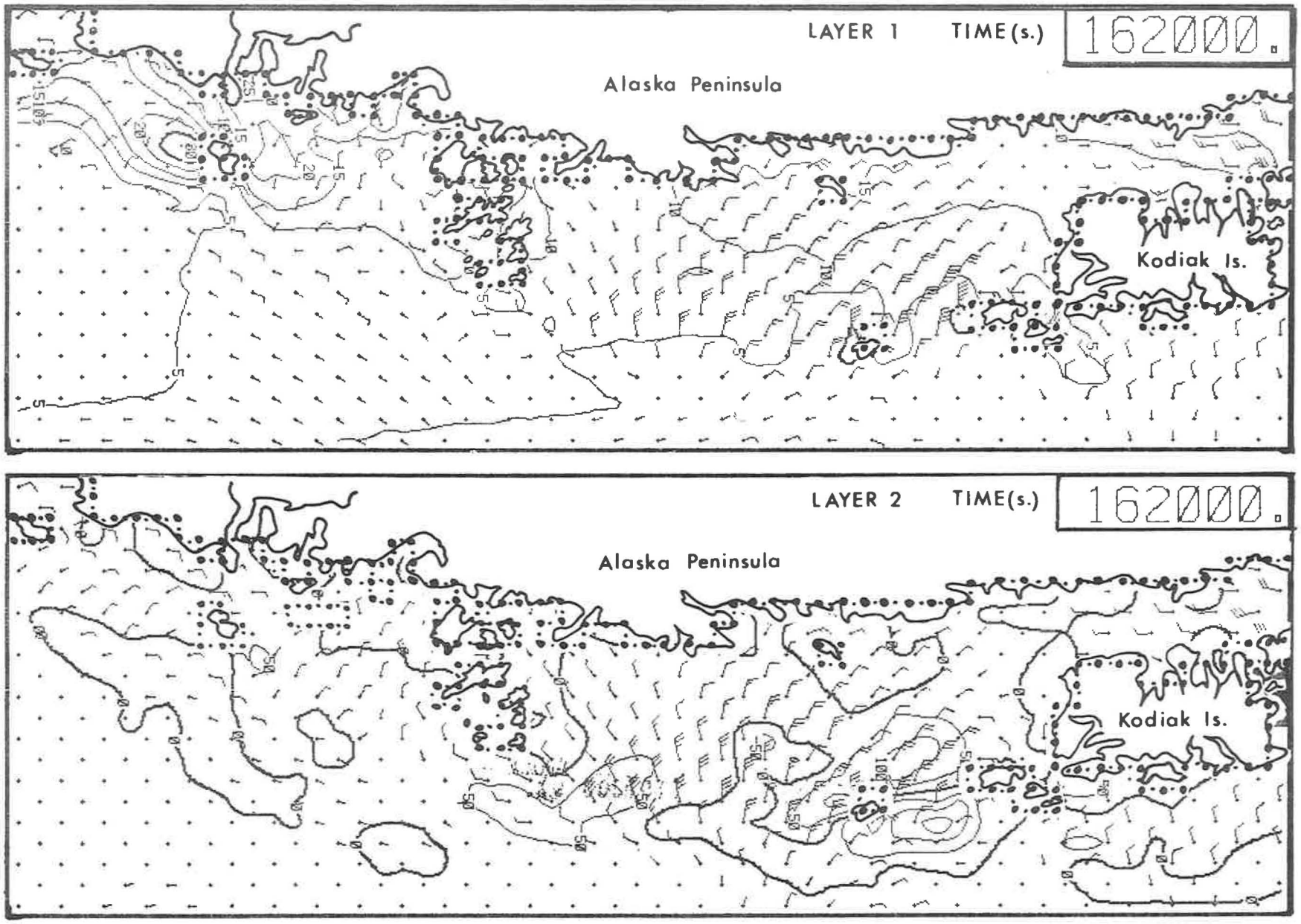

13. Case 1, currents (cm/s) and tidal heights (cm) for layers 1 and 2 at 45 hours (162000 s).

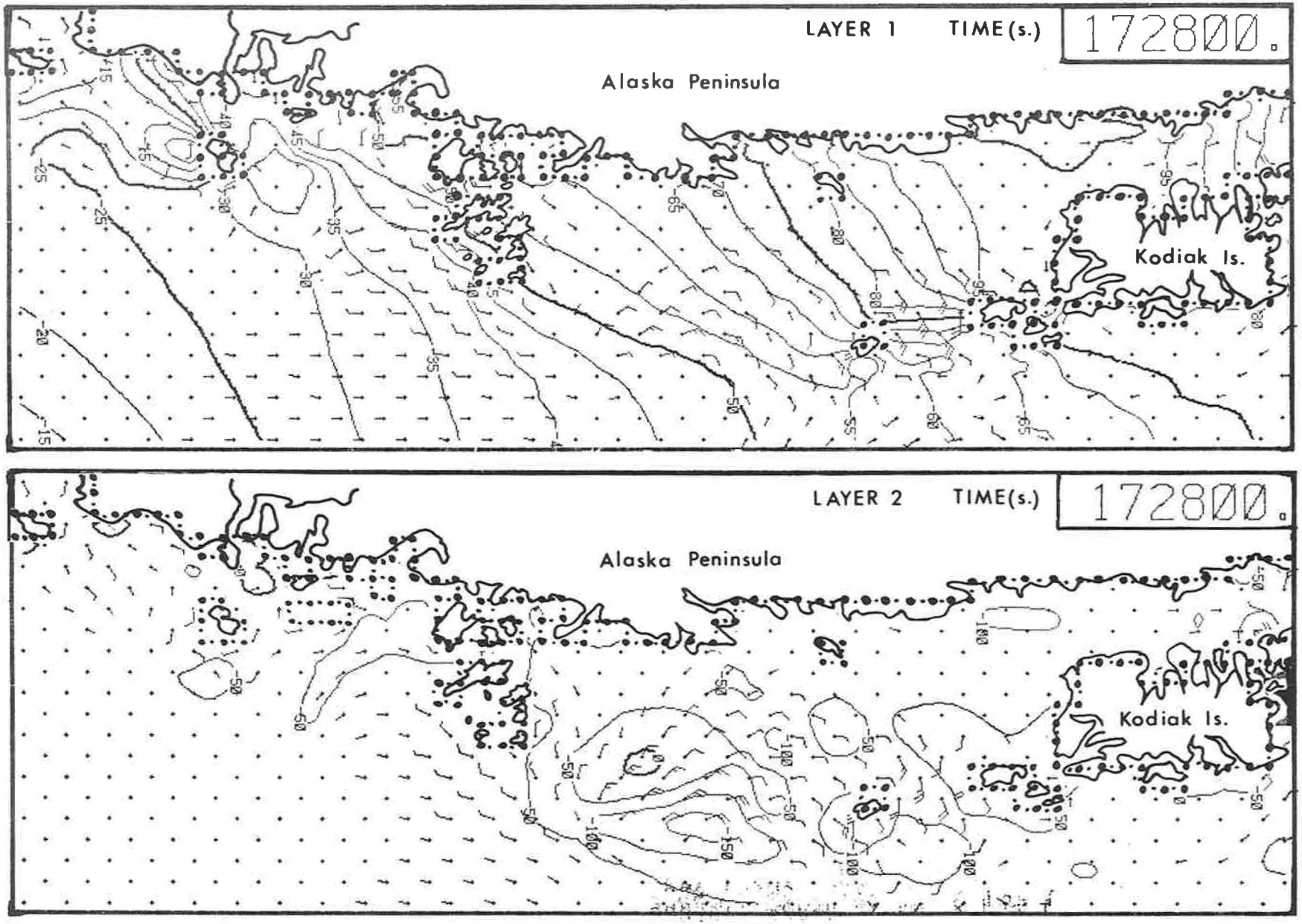

14. Case 1, currents (cm/s) and tidal heights (cm) for layers 1 and 2 at 48 hours (172800 s).

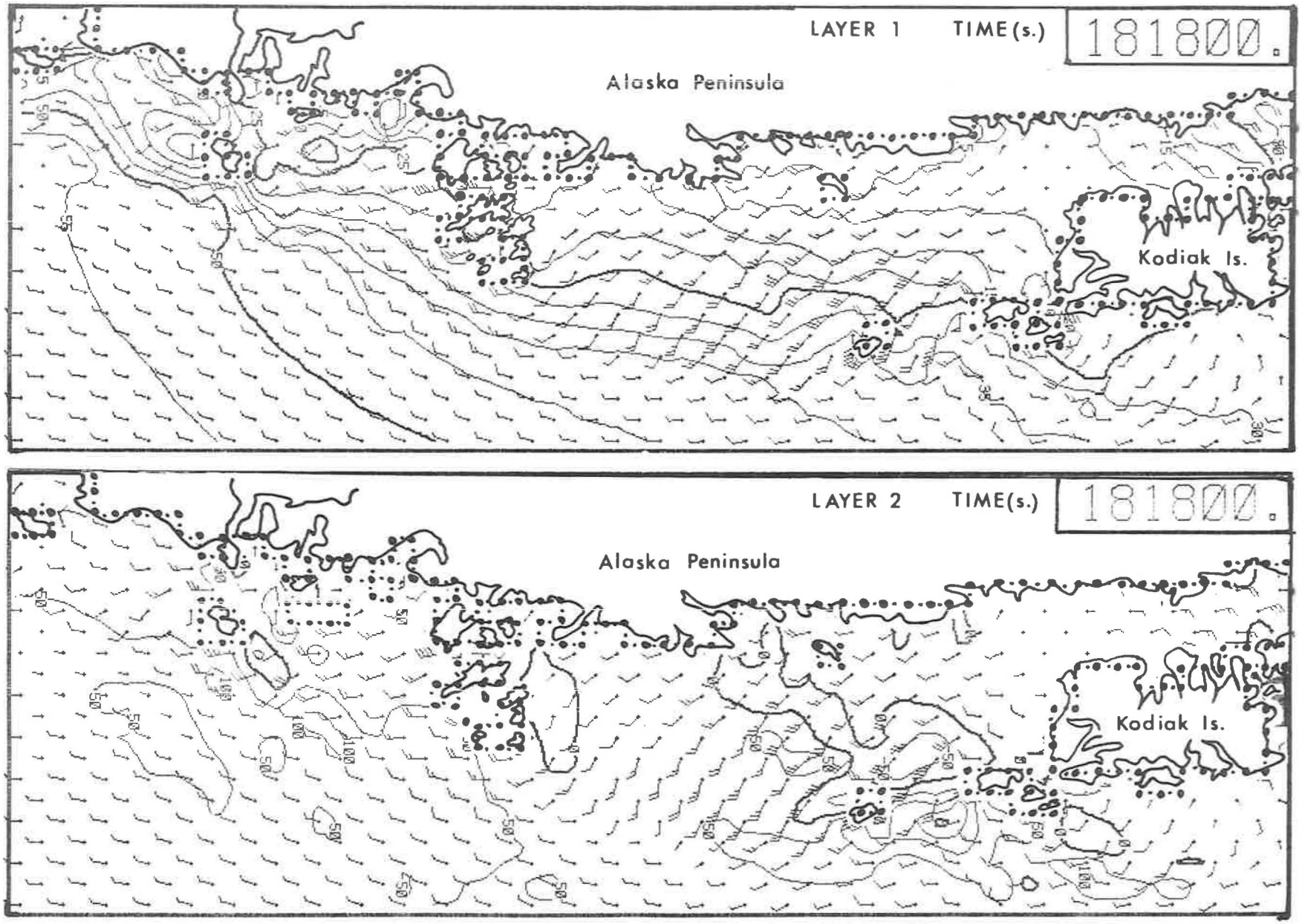

15. Case 1, currents (cm/s) and tidal heights (cm) for layers 1 and 2 at 50 1/2 hours (181800 s).

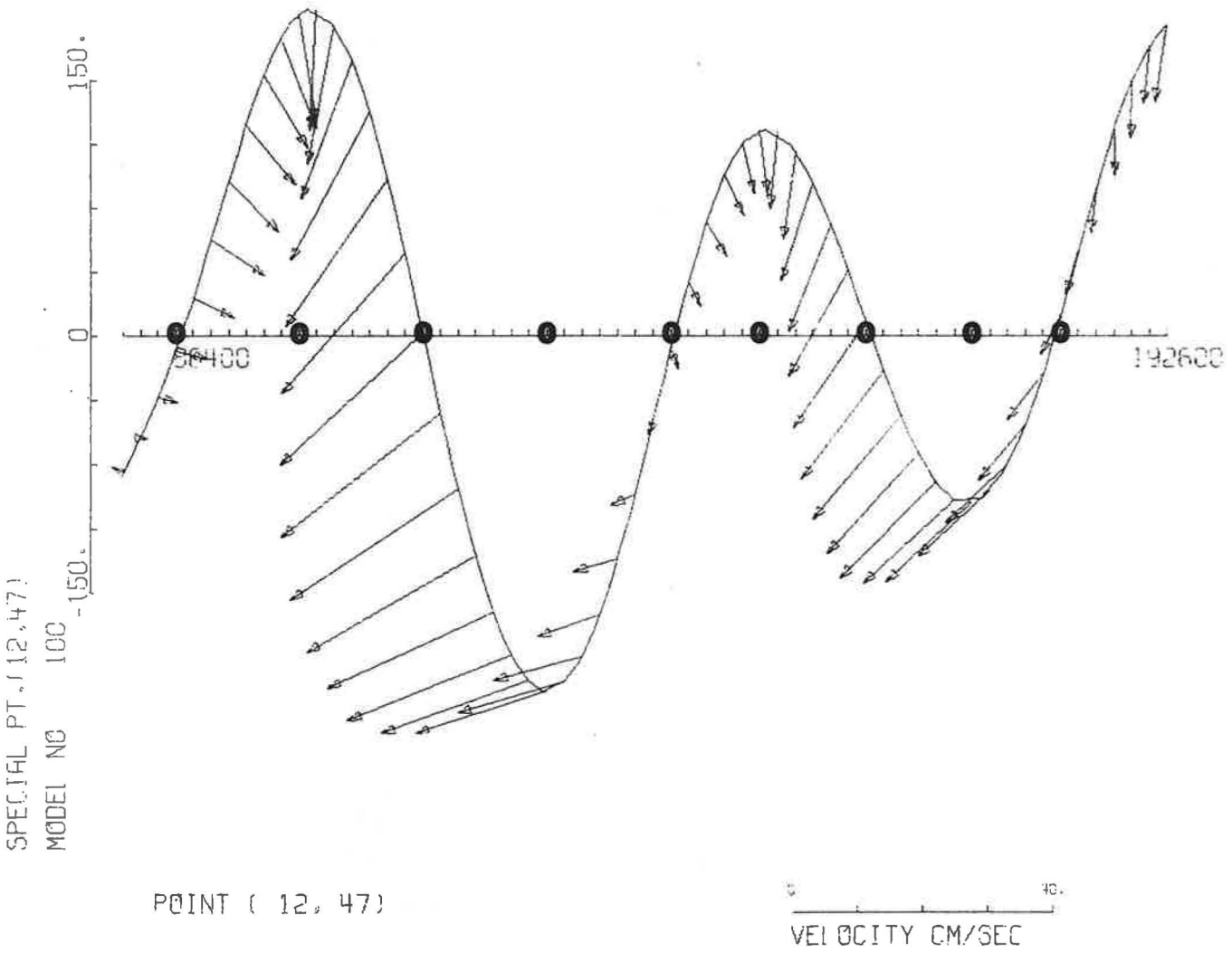

16. TIDAL HEIGHTS AND CURRENTS WITH NW WINDS
LAYER3, OPTIMIZED H-N MODEL FOR B.L.M. GULF OF ALASKA, WESTERN GRID.

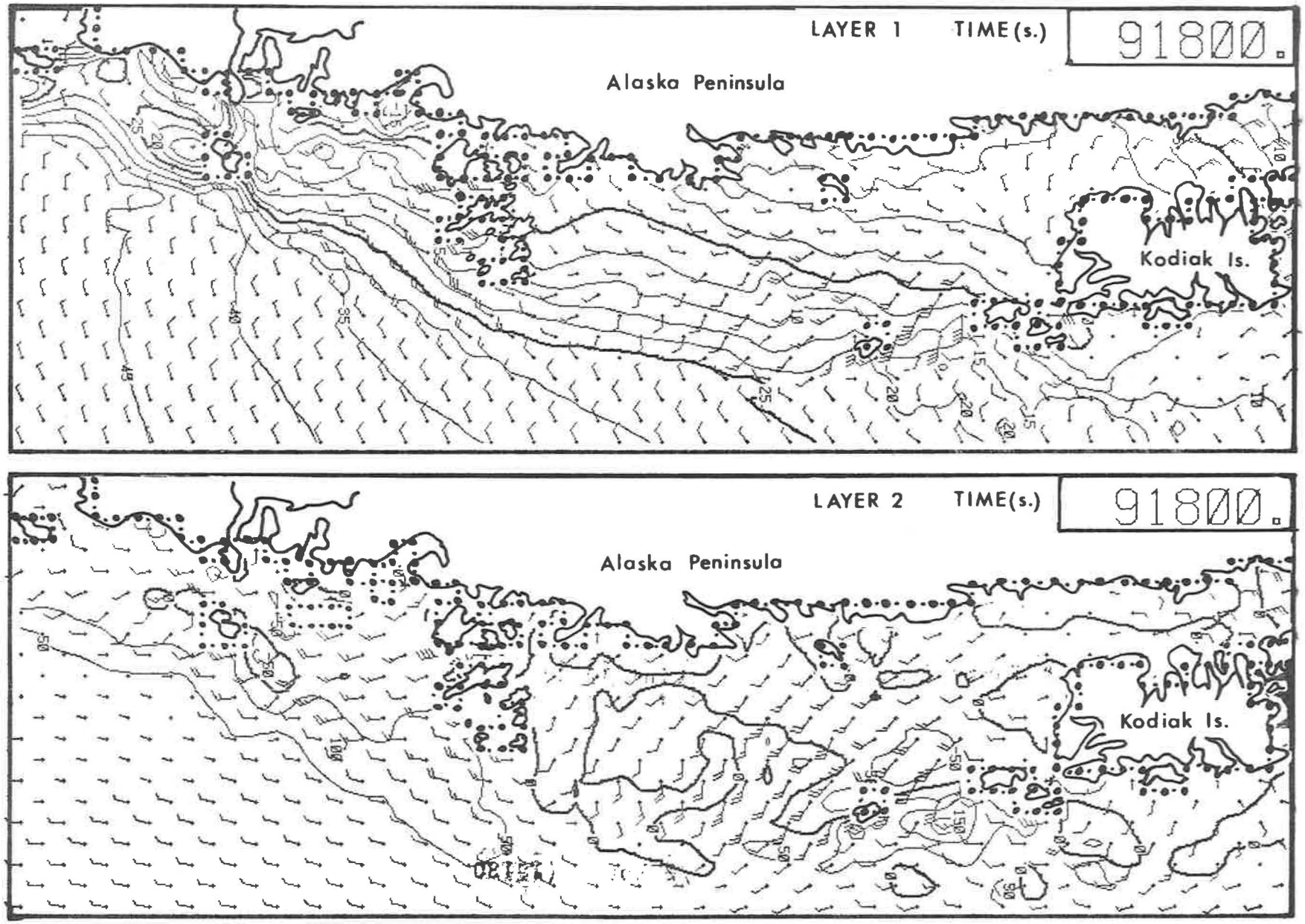

17. Case 2, currents (cm/s) and tidal heights (cm) for layers 1 and 2 at 25 1/2 hours (91800 s).

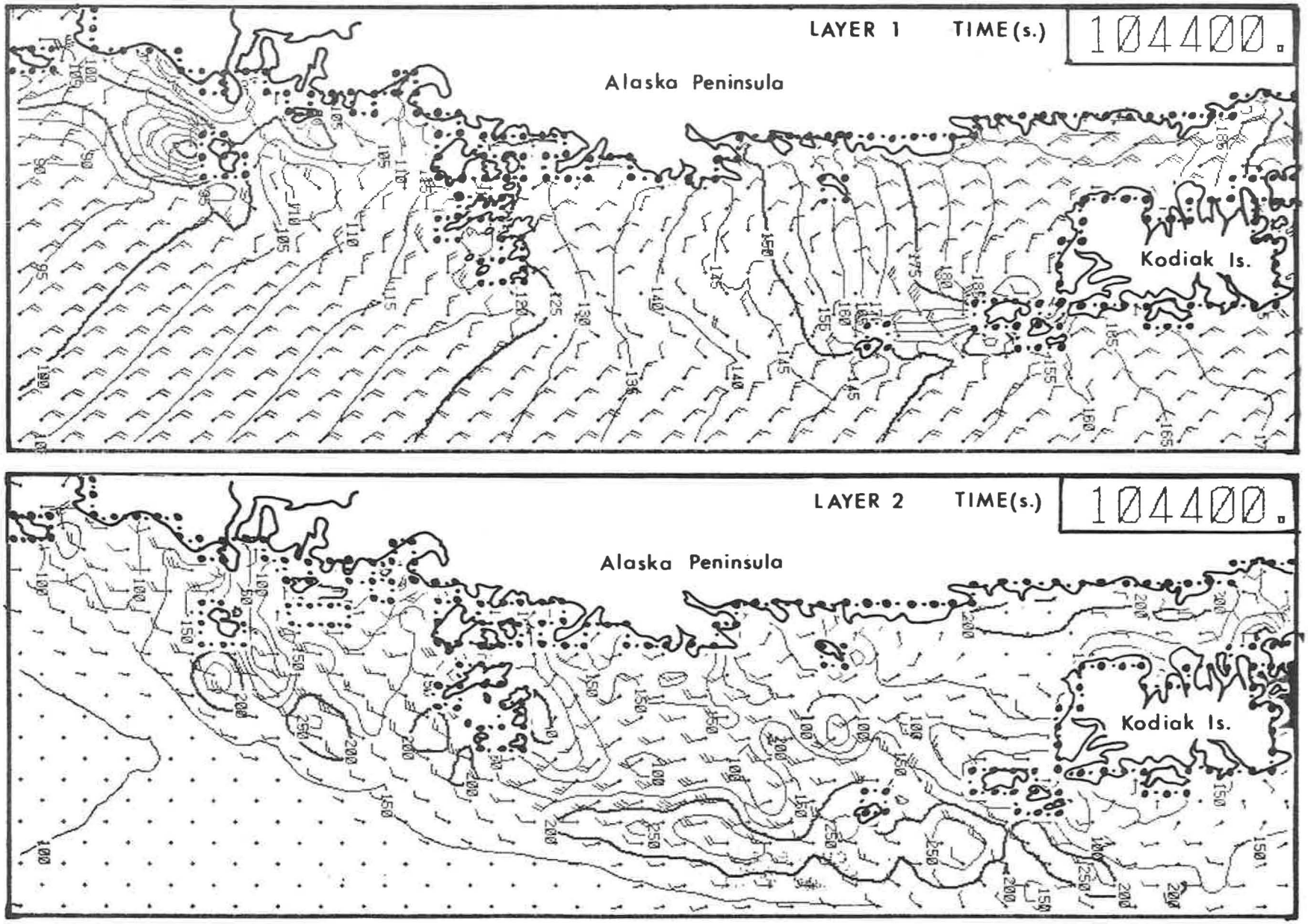

18. Case 2, currents (cm/s) and tidal heights (cm) for layers 1 and 2 at 29 hours (104400 s).

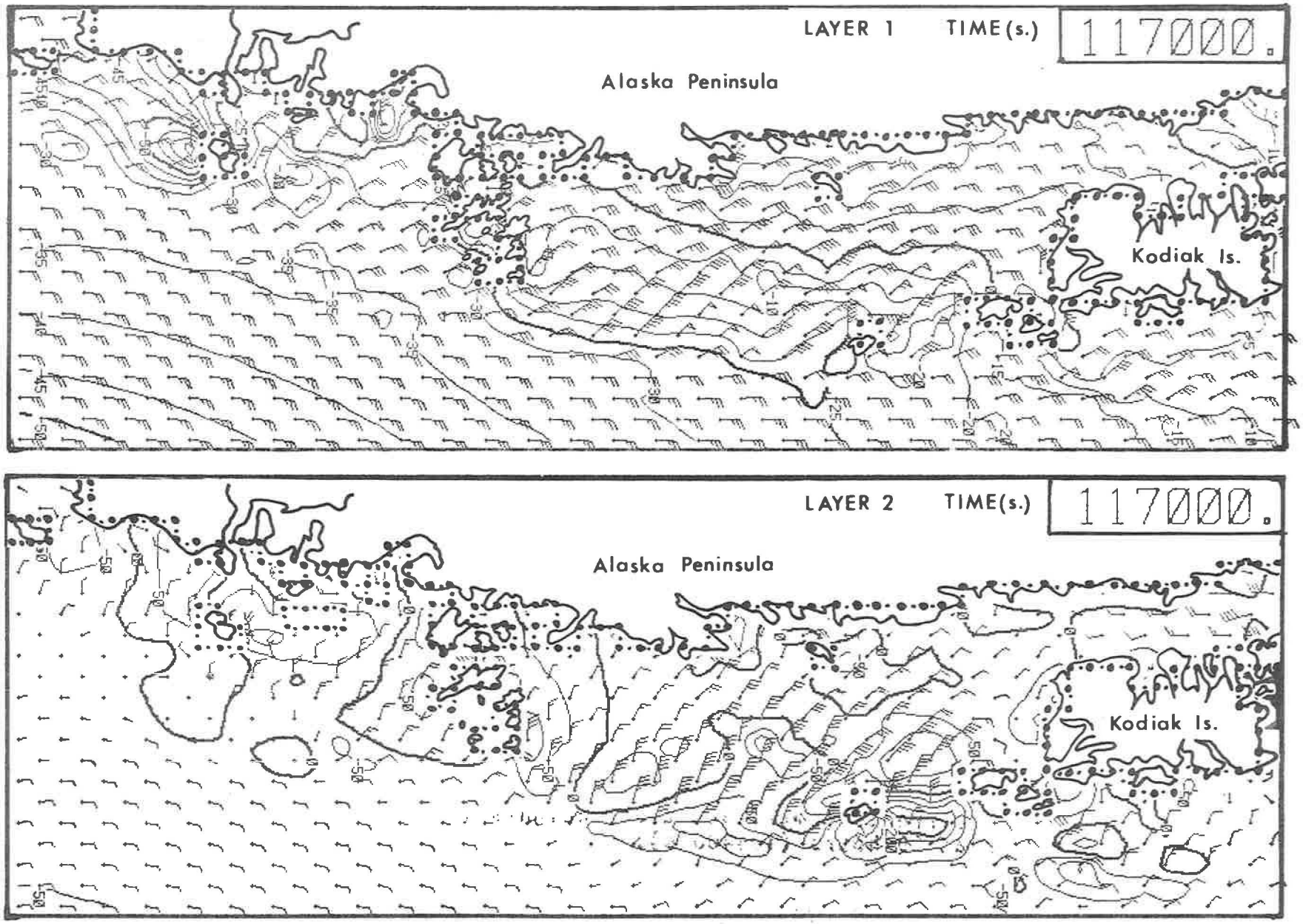

19. Case 2, currents (cm/s) and tidal heights (cm) for layers 1 and 2 at 32 1/2 hours (117000 s).

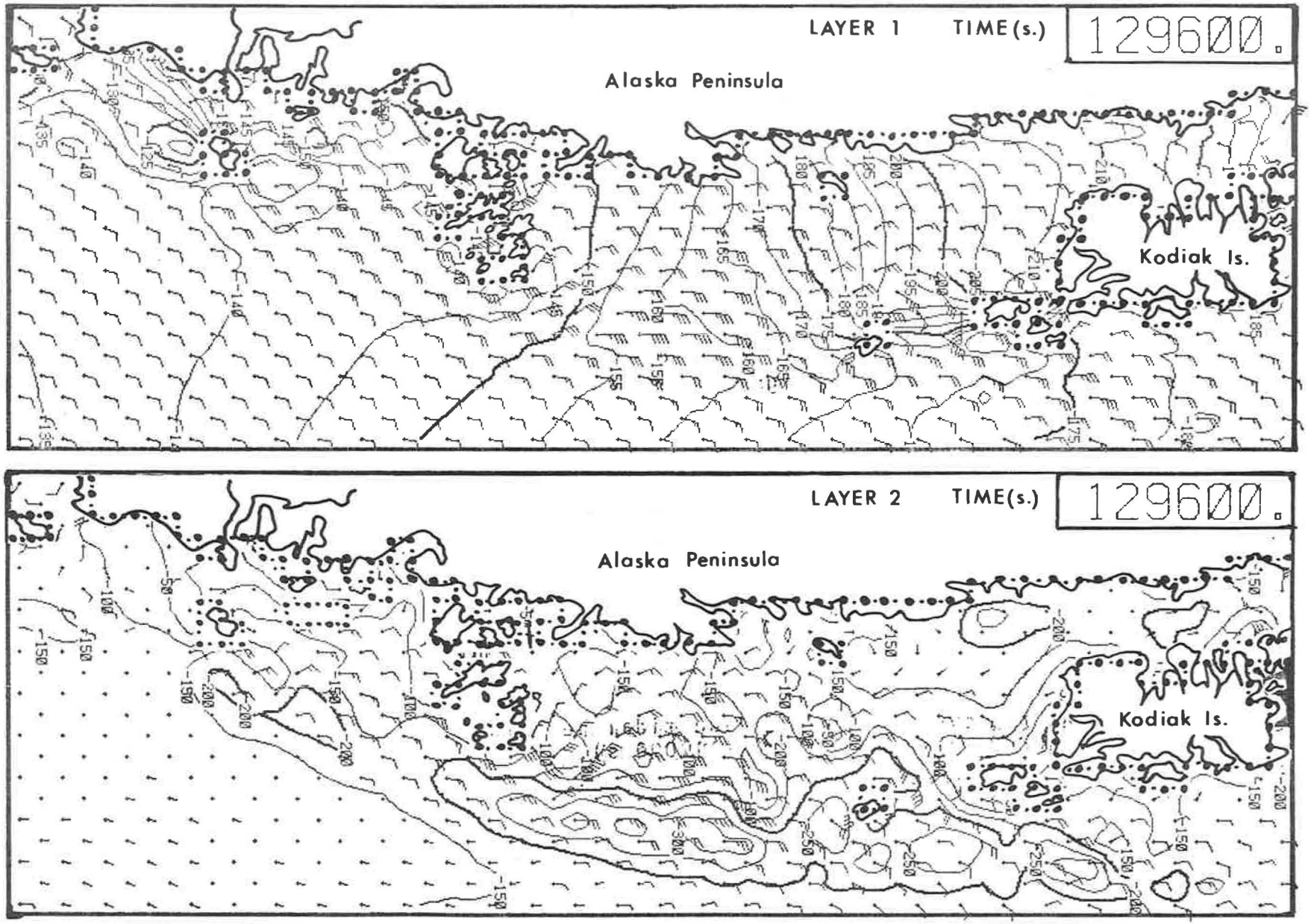

20. Case 2, currents (cm/s) and tidal heights (cm) for layers 1 and 2 at 36 hours (129600 s).

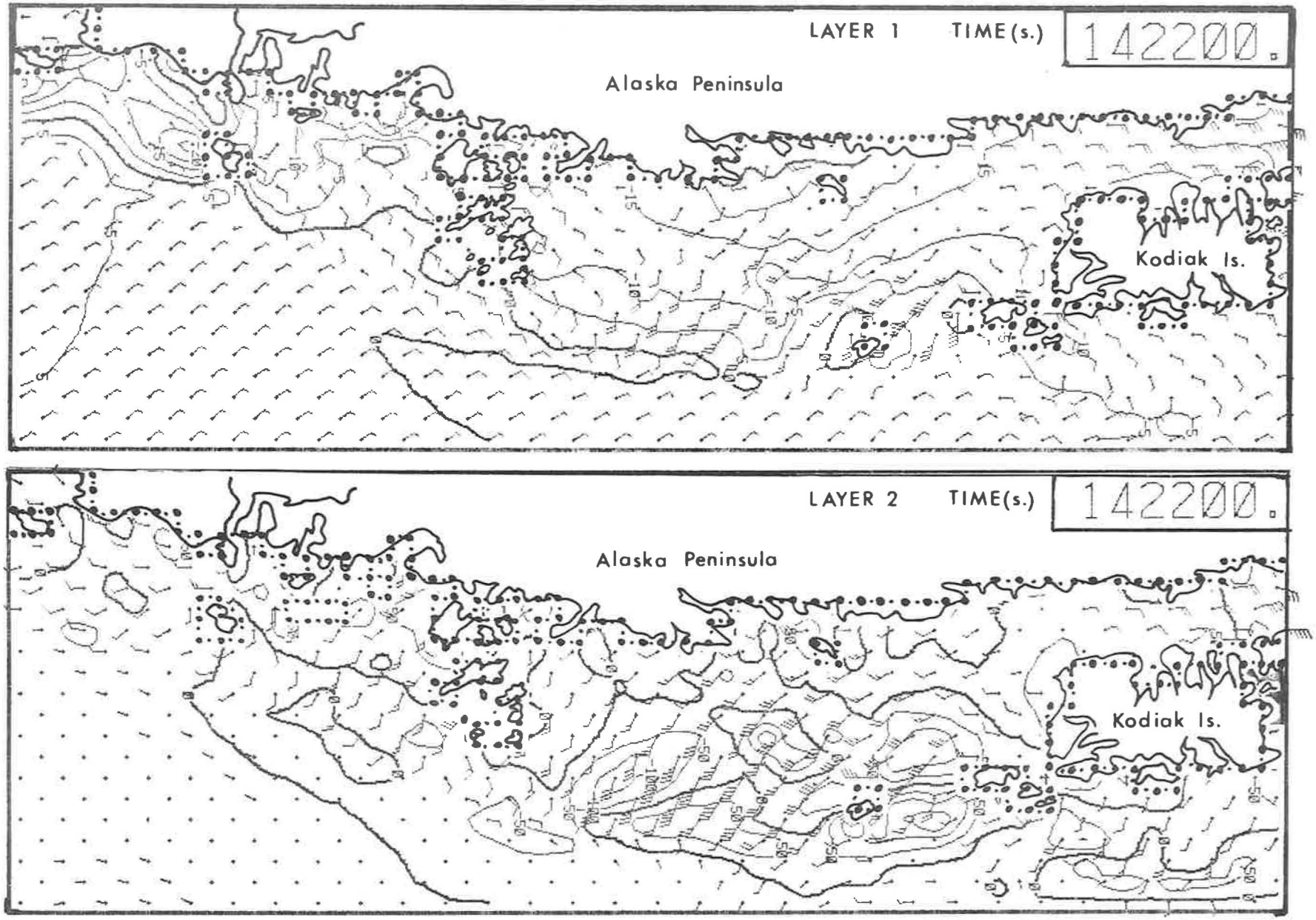

21. Case 2, currents (cm/s) and tidal heights (cm) for layers 1 and 2 at 39 1/2 hours (142200 s).

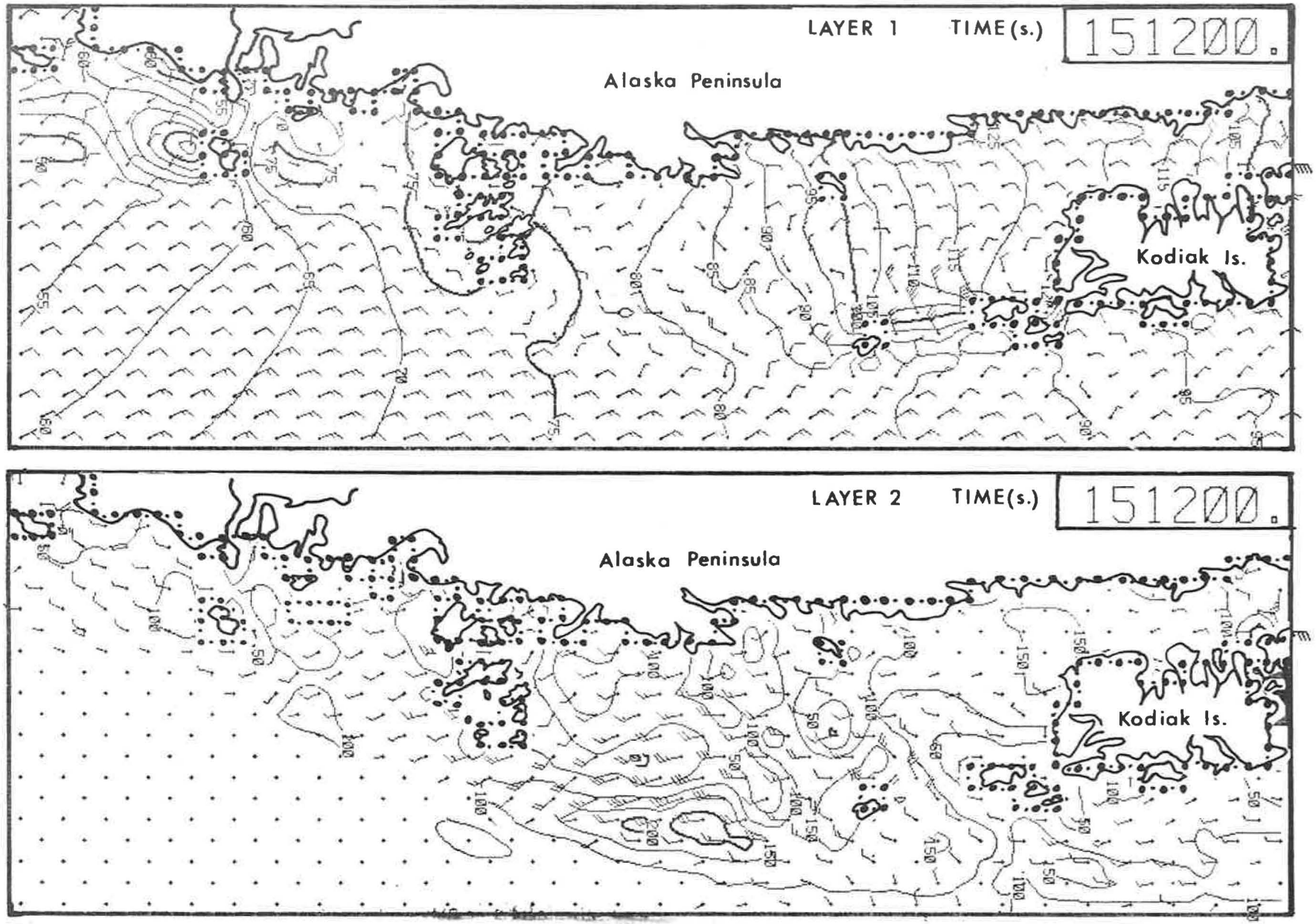

22. Case 2, currents (cm/s) and tidal heights (cm) for layers 1 and 2 at 42 hours (151200 s).

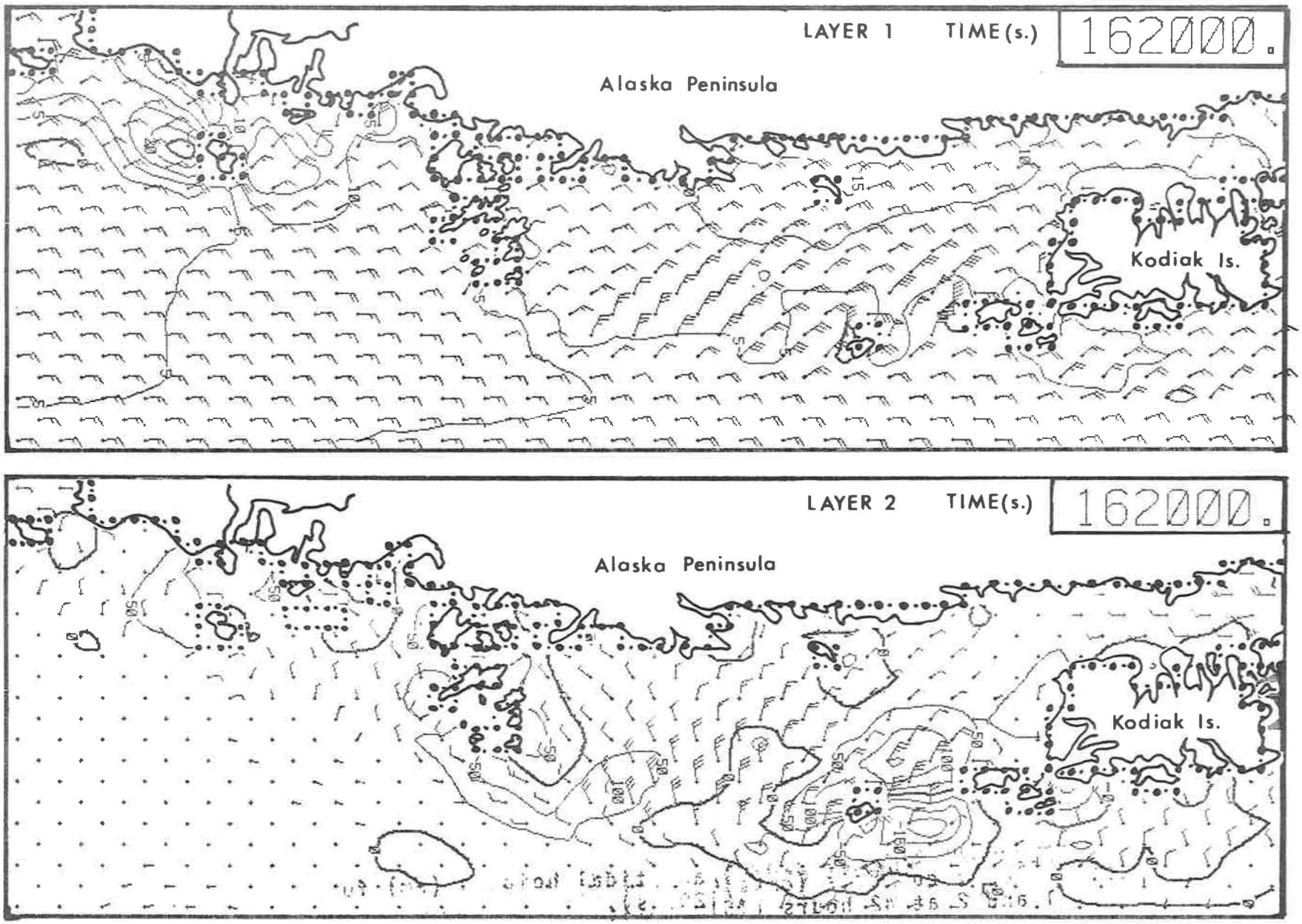

23. Case 2, currents (cm/s) and tidal heights (cm) for layers 1 and 2 at 45 hours (162000 s).

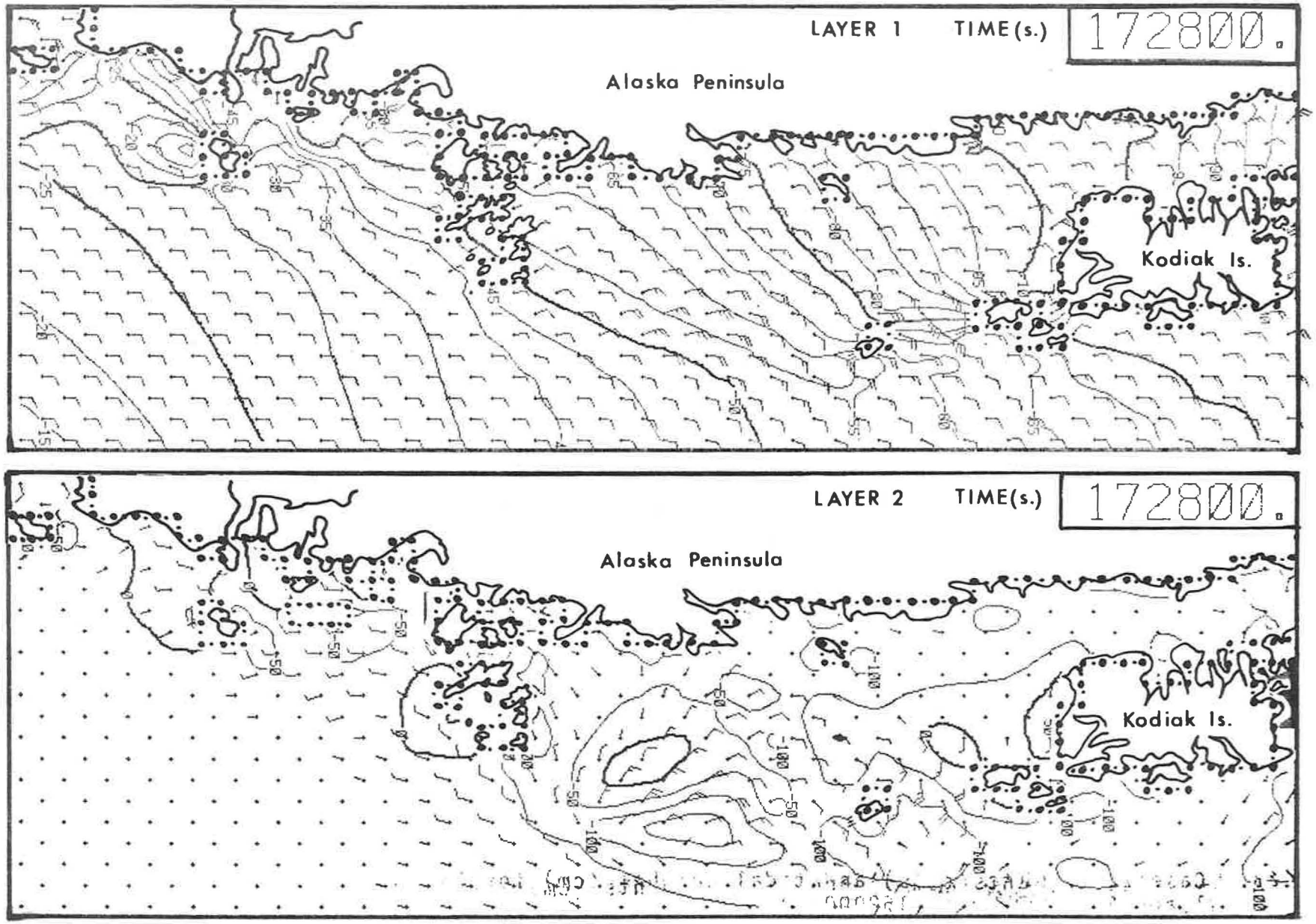

24. Case 2, currents (cm/s) and tidal heights (cm) for layers 1 and 2 at 48 hours (172800 s).

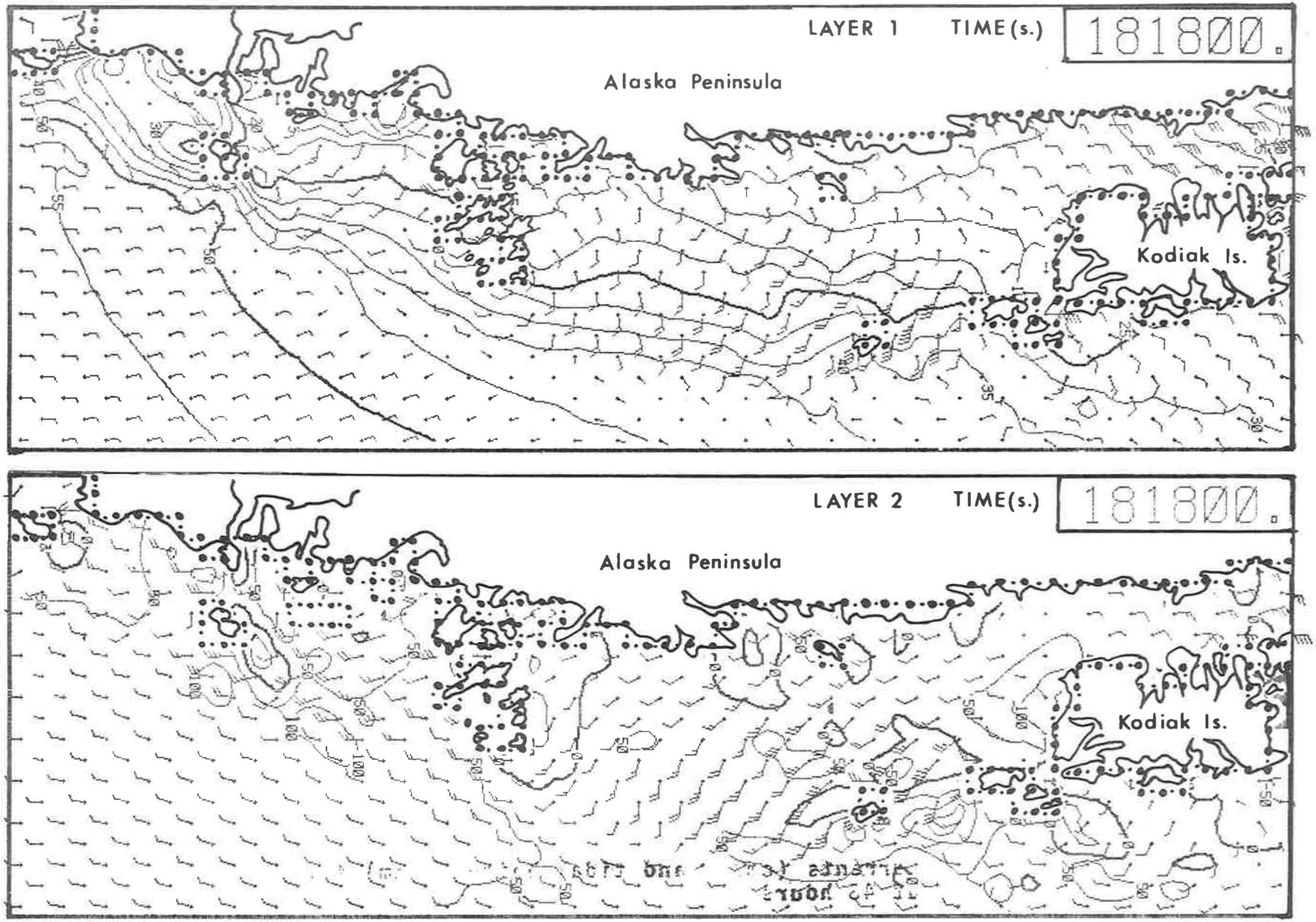

25. Case 2, currents (cm/s) and tidal heights (cm) for layers 1 and 2 at 50 1/2 hours (181800 s).

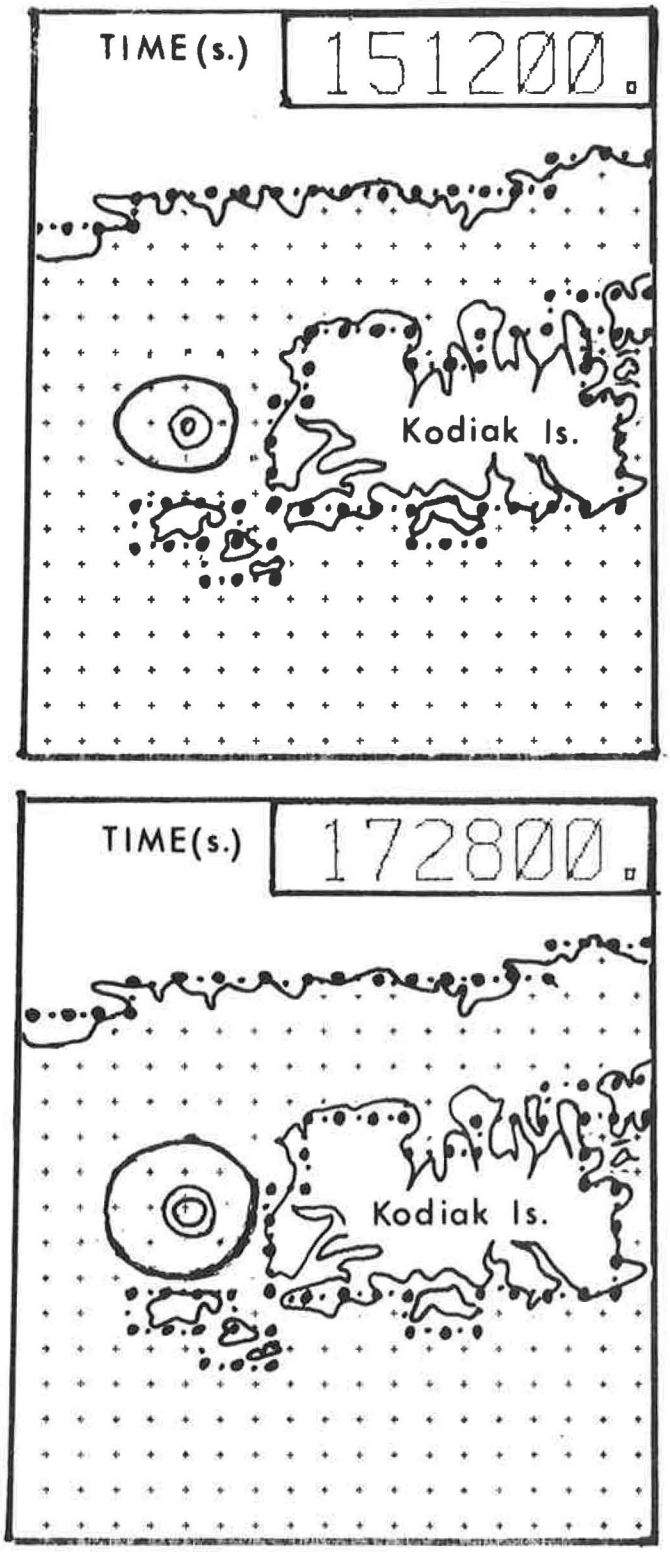

26. Case 1, pollutant distribution (arbitrary units) at 42 hours (151200 s) and 48 hours (172800 s) after starting continuous source at 29 hours (104400 s).

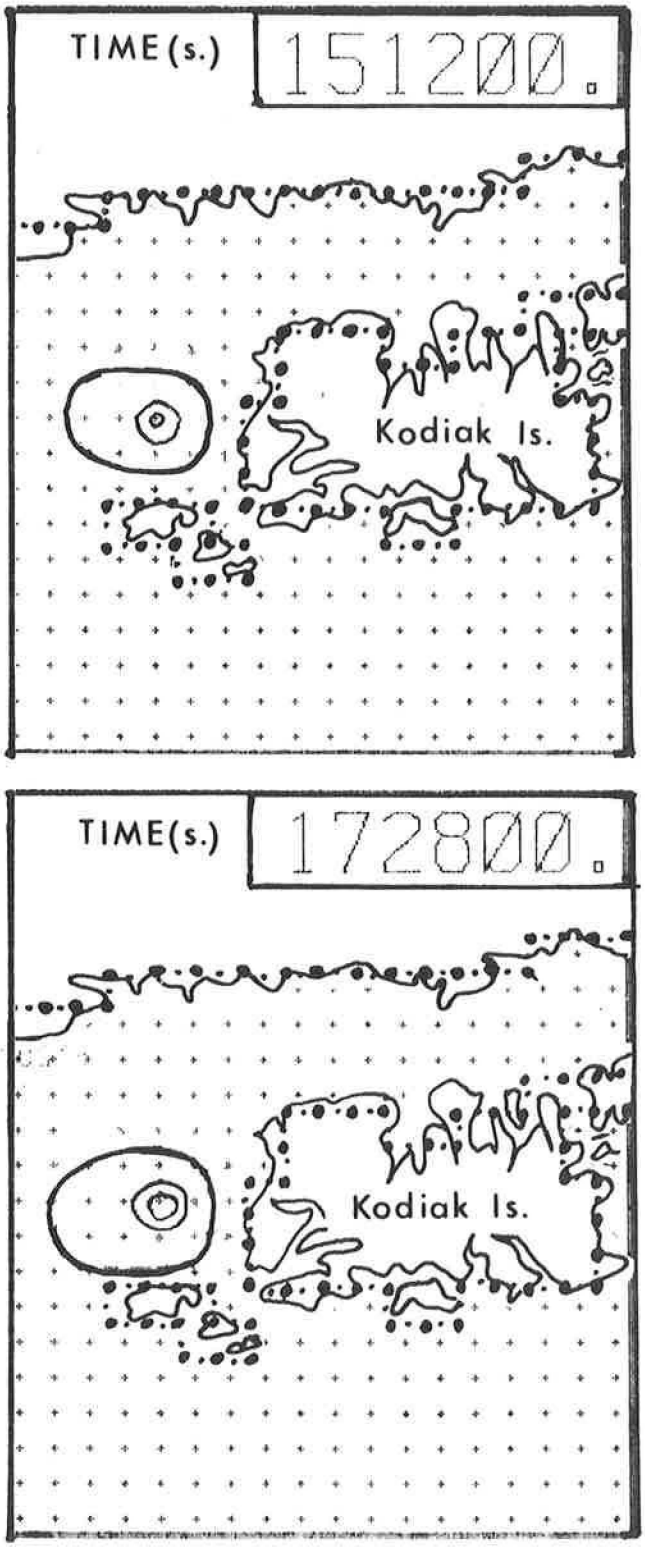

27. Case 2, pollutant distribution (arbitrary units) at 42 hours (151200 s) and 48 hours (172800 s) after starting continuous source at 29 hours (104400 s).